DMD Fast Forward. Published on September 6, 2019 as DOI: 10.1124/dmd.119.088823
This article has not been copyedited and formatted. The final version may differ from this version.

Title: Inter-Individual Variation in CYP3A Activity Influences Lapatinib Bioactivation

Authors: Jennifer E. Bissada, Vivian Truong, Arsany A. Abouda, Kahari J. Wines, Rachel D. Crouch, and Klarissa D. Jackson

Department of Pharmaceutical Sciences, Lipscomb University College of Pharmacy and Health Sciences, Nashville, Tennessee (J.E.B., V.T., A.A.A., K.J.W., R.D.C.); *Department of Pharmacology, Vanderbilt University School of Medicine, Nashville, Tennessee (R.D.C.); Division of Pharmacotherapy and Experimental Therapeutics, UNC Eshelman School of Pharmacy, University of North Carolina at Chapel Hill, Chapel Hill, North Carolina (K.D.J.)*

Running Title: CYP3A Activity and Lapatinib Bioactivation

Address Correspondence to:

Klarissa D. Jackson, Ph.D., UNC Eshelman School of Pharmacy, University of North Carolina at Chapel Hill, 3320 Kerr Hall, CB# 7569, Chapel Hill, NC 27599-7569.Phone: (919) 962-5551. Email: klarissa.jackson@unc.edu

Document Summary:

Number of Text Pages	50
Number of Tables	1
Number of Figures	11
Number of References	58
Number of Words in Abstract	250
Number of Words in Significance Statement	74
Number of Words in Introduction	780
Number of Words in Discussion	1596

Abbreviations Used: AO, aldehyde oxidase; BCRP, breast cancer resistance protein; CYP, cytochrome P450; DMSO, dimethyl sulfoxide; EGFR, epidermal growth factor receptor 1; HER2, human epidermal growth factor receptor 2; HLA, human leukocyte antigen; HLM, human liver microsomes; HPLC, high performance liquid chromatography; M1, debenzylated lapatinib; KHB, Krebs-Henseleit buffer; LC-MS/MS, liquid chromatography-tandem mass spectrometry; MRM, multiple reaction monitoring; OATP1B1, organic anion transporting polypeptide 1B1; Pgp, P-glycoprotein, ABCB1; XO, xanthine oxidase

Abstract

Lapatinib is a dual tyrosine kinase inhibitor associated with rare but potentially severe idiosyncratic hepatotoxicity. We have previously shown that cytochromes P450 (CYP) 3A4 and CYP3A5 quantitatively contribute to lapatinib bioactivation leading to formation of a reactive, potentially toxic quinoneimine. CYP3A5 is highly polymorphic; however, the impact of CYP3A5 polymorphism on lapatinib metabolism has not been fully established. The goal of this study was to determine the effect of *CYP3A5* genotype and individual variation in CYP3A activity on the metabolic activation of lapatinib using human-relevant in vitro systems. Lapatinib metabolism was examined using *CYP3A5*-genotyped human liver microsomes and cryopreserved human hepatocytes. CYP3A and CYP3A5-selective activities were measured in liver tissues using probe substrates midazolam and T-5 (T-1032), respectively, to evaluate the correlation between enzymatic activity and lapatinib metabolite formation. Drug metabolites were measured by HPLC – tandem mass spectrometry. Further, the relative contributions of CYP3A4 and CYP3A5 to lapatinib *O*-debenzylation were estimated using selective chemical inhibitors of CYP3A. The results from this study demonstrated that lapatinib *O*-debenzylation and quinoneimine-GSH conjugate formation were highly correlated with hepatic CYP3A activity, as measured by midazolam 1´-hydroxylation. CYP3A4 played a dominant role in lapatinib bioactivation in all liver tissues evaluated. The CYP3A5 contribution to lapatinib bioactivation varied by individual donor and was dependent on CYP3A5 genotype and activity. CYP3A5 contributed approximately 20-42% to lapatinib *O*-debenzylation in livers from CYP3A5 expressers. These findings indicate that individual CYP3A activity, not *CYP3A5* genotype alone, is a key

determinant of lapatinib bioactivation and likely influences exposure to reactive metabolites.

Significance Statement:

This is the first study to examine the effect of *CYP3A5* genotype, total CYP3A activity, and CYP3A5-selective activity on lapatinib bioactivation in individual human liver tissues. The results of this investigation indicate that lapatinib bioactivation via oxidative *O*-debenzylation is highly correlated with total hepatic CYP3A activity, and not *CYP3A5* genotype alone. These findings provide insight into the individual factors, namely CYP3A activity, that may affect individual exposure to reactive, potentially toxic metabolites of lapatinib.

DMD Fast Forward. Published on September 6, 2019 as DOI: 10.1124/dmd.119.088823
This article has not been copyedited and formatted. The final version may differ from this version.

Introduction

Lapatinib was the first orally active small molecule dual inhibitor of epidermal growth factor receptor (EGFR) and human epidermal growth factor receptor 2 (HER2) approved (2007) for the treatment of advanced or metastatic HER2-positive breast cancer (Rusnak et al., 2001; Lackey, 2006; Moy et al., 2007). Clinical use of lapatinib is limited due to severe, sometimes fatal idiosyncratic hepatotoxicity (Peroukides et al., 2011; Spraggs et al., 2011; Moy et al., 2009; Azim et al., 2013; Goss et al., 2013; Gomez et al., 2008). Lapatinib-induced liver injury is thought to have an immune component due to the association of specific human leukocyte antigen (HLA) risk alleles with the incidence of hepatotoxicity (Spraggs et al., 2011; Spraggs et al., 2012; Schaid et al., 2014; Parham et al., 2015); however, the mechanisms of the lapatinib-induced liver injury are still poorly defined.

Metabolic activation of lapatinib by cytochrome P450 (CYP) 3A enzymes has been implicated in the development of lapatinib-induced liver injury (Castellino et al., 2012). Lapatinib is extensively metabolized by CYP3A4 and CYP3A5 via oxidative *O*-debenzylation to a *para*-hydroxy aniline metabolite, debenzylated lapatinib (M1); this metabolite can be further oxidized to a reactive quinoneimine (Teng et al., 2010; Castellino et al., 2012). Glutathione (GSH) and other thiol conjugates of the quinoneimine have been detected in vitro in incubations with recombinant P450s, human liver microsomes, and/or hepatic cell cultures (Teng et al., 2010; Chan et al., 2012; Hardy et al., 2014; Towles et al., 2016). CYP3A4 induction by dexamethasone and rifampin enhanced the cytotoxicity of lapatinib in HepaRG cells and was correlated

with increased reactive metabolite generation (Hardy et al., 2014). Moreover, debenzylated lapatinib was more cytotoxic to HepaRG cells compared to the parent drug (Hardy et al., 2014). In the clinical setting, the risk of lapatinib-induced hepatotoxicity was increased in breast cancer patients taking dexamethasone and lapatinib compared to patients treated with lapatinib alone (Teo et al., 2012). These observations suggest at least a partial role of lapatinib metabolites in mediating hepatotoxicity.

We have previously shown that both CYP3A4 and CYP3A5 contribute to lapatinib bioactivation (Towles et al., 2016); however, the impact of *CYP3A5* polymorphism on lapatinib metabolism has not been fully established (Chan et al., 2014; Ho et al., 2015). CYP3A5 shares 84% sequence identity with CYP3A4 (Aoyama et al., 1989), and the enzymes share overlapping substrates (Wrighton and Stevens, 1992; Huang et al., 2004). While CYP3A4 is abundantly expressed in human liver and intestine, CYP3A5 is highly polymorphic (Hustert et al., 2001; Kuehl et al., 2001; Lamba et al., 2002; Lin et al., 2002). The presence of the *CYP3A5*1* wild-type allele leads to expression of high levels of functional CYP3A5 protein, whereas the most common CYP3A5 variant allele **3* results in low to undetectable levels of CYP3A5 due to improper mRNA splicing (Kuehl et al., 2001). The *CYP3A5*3/*3* genotype is most frequent among individuals of European descent (70-90%); 30-40% of Asians, and 50-70% of people of African descent carry at least one *CYP3A5*1* allele (CYP3A5 expressers) (Hustert et al., 2001; Kuehl et al., 2001; Lamba et al., 2002). In CYP3A5 expressers, CYP3A5 may contribute significantly to overall CYP3A content and catalytic activity (Kuehl et al., 2001; Huang et al., 2004). An increasing number of examples

indicate that *CYP3A5* polymorphism can impact the metabolism and pharmacokinetics of CYP3A substrates, including tacrolimus (Hesselink et al., 2003; Birdwell et al., 2015), alfentanil (Klees et al., 2005), vincristine (Dennison et al., 2007), and maraviroc (Lu et al., 2012; Lu et al., 2014).

Recent tools have been developed to differentiate between CYP3A4 and CYP3A5 contributions to drug metabolism. CYP3cide and SR-9186 are CYP3A4-selective chemical inhibitors (Li et al., 2012; Walsky et al., 2012). The difference between inhibition by CYP3cide (CYP3A4-selective inactivator) and ketoconazole (CYP3A pan inhibitor) has been used as an approach to estimate CYP3A5 contributions to metabolism of multiple CYP3A substrates (Tseng et al., 2014; Towles et al., 2016; Zientek et al., 2016; Tseng et al., 2018). Further, *N*-oxidation of T-5 was identified as a selective marker reaction to measure CYP3A5 activity (Li et al., 2014). This marker reaction can now be used to selectively evaluate the CYP3A5 genotype – phenotype relationship with respect to enzyme expression and activity.

The goal of the present study was to determine the effect of *CYP3A5* genotype and CYP3A activity on the metabolic activation of lapatinib in genotyped human liver tissues. We hypothesized that CYP3A5 polymorphism would have a significant impact on lapatinib *O*-debenzylation and reactive metabolite formation. Studies were done to 1) examine lapatinib metabolism in *CYP3A5*-genotyped human liver microsomes and cryopreserved human hepatocytes, 2) assess the correlation between metabolite formation and CYP3A and CYP3A5-selective activity, and 3) estimate the relative contributions of CYP3A4 and CYP3A5 to lapatinib *O*-debenzylation.

DMD Fast Forward. Published on September 6, 2019 as DOI: 10.1124/dmd.119.088823
This article has not been copyedited and formatted. The final version may differ from this version.

Materials and Methods

Chemicals and reagents

Lapatinib (free base; L-4899) was purchased from LC Laboratories (Woburn, MA). Debenzylated lapatinib (M1) was chemically synthesized according to the methods described previously (Teng et al., 2010). Deuterium-labeled *O*-debenzylated lapatinib ([$^2H_4$]*O*-debenzylated lapatinib, d_4-Lap-OH, C-10309) was chemically synthesized and provided by CoNCERT Pharmaceuticals (Lexington, MA), as described previously (Towles et al., 2016). Lapatinib stock solutions were prepared in dimethyl sulfoxide (DMSO), and working solutions were prepared in 1:9 DMSO/acetonitrile (v/v). Reduced glutathione (GSH), allopurinol, hydralazine hydrochloride, and O^6-benzylguanine were purchased from Sigma Aldrich. Midazolam, 1´-hydroxymidazolam, and d_4-1´-hydroxymidazolam were purchased from Cerilliant. T-5 (T-1032, [methyl 2-(4-aminophenyl)-1-oxo-7-(pyridin-2-ylmethoxy)-4- (3,4,5-trimethoxyphenyl)-1,2-dihydroisoquinoline-3-carboxylate]) (Li et al., 2014) and T-5 *N*-oxide standards were generous gifts from Michael Cameron (Scripps Institute, Florida). Stock solutions were prepared in DMSO, diluted in 1:9 DMSO/acetonitrile (v/v) working solutions, and stored at -20°C.

An NADPH-regenerating system, consisting of Solution A (26 mM NADP+, 66 mM glucose 6-phosphate, 66 mM $MgCl_2$ in water) and Solution B (40 U/ml glucose 6-phosphate dehydrogenase in 5 mM sodium citrate), was purchased from Corning Life Sciences. OptiThaw Media Kit (Product #: K8000) was purchased from XenoTech, LLC.

InVitroGRO Krebs-Henseleit buffer (KHB) Medium (Product #: Z99074) was purchased from BioreclamationIVT (BioIVT).

Human liver subcellular fractions and cryopreserved hepatocytes

Human liver microsomes: Pooled human liver microsomes from 150 donors, mixed gender, (Corning, lot number 38291) were purchased from Corning Life Sciences. Single-donor human liver microsomal samples from 12 donors genotyped for *CYP3A5* were purchased from Corning Life Sciences and XenoTech, LLC. Donors included eight males (M) and four females (F), ages 26-66 years old. *CYP3A5* genotype reported by the company for each donor was as follows: *CYP3A5*1/*1* donors were HH860(F), HH867(M), HH785(M), 710272(F); *CYP3A5*1/*3* donors were HH757(M), HH868(M), 710232(F); *CYP3A5*3/*3* donors were HH189(F), HH507(M), 710252(M), 710253(M), 710237(M).

Human liver S9 fraction: Human liver S9 fraction pooled from 10 donors (mixed gender) was prepared according to procedures described previously (Towles et al., 2016). Commercially available human liver S9 fraction pooled from 20 donors (mixed gender) was purchased from XenoTech (catalog number H0606.S9(AX), lot number 1710129).

Cryopreserved human hepatocytes: Cryopreserved human hepatocytes pooled from five donors (mixed gender) were purchased from BioIVT. *CYP3A5*-genotyped cryopreserved human hepatocytes pooled from three donors (mixed gender) were purchased from XenoTech. Lot HPCH.3A5.HA with genotype *CYP3A5*1/*1* was classified as “high activity” (donors 979, 1019, 1057; two males, one female); lot

HPCH.3A5.MA with genotype *CYP3A5*1/*3* was classified as "medium activity" (donors 1173, 1186, 1203; one male, two females); and lot HPCH.3A5.NA. with genotype *CYP3A5*3/*3* was classified as "no activity" (donors 1196, 1207, 1211; one male, two females). CYP3A activity in each pooled lot was measured by XenoTech using testosterone 6β-hydroxylation and midazolam 1´-hydroxylation as marker reactions.

Single-donor cryopreserved human hepatocytes from fifteen donors genotyped for *CYP3A5* were purchased from BioIVT. Hepatocyte donors included eight males and seven females, ages 39-68 years old. *CYP3A5*1/*1* donors were RSA(M), RQM(F); *CYP3A5*1/*3* donors were GTD(M), DGW(M), ZUJ(M), KCM(F), OWY(F); *CYP3A5*3/*3* donors were YUA(M), ORM(M), EFF(M), BTA(M), OTH(F), CBD(F), XUA(F), and JYS(F).

Measurement of CYP3A and CYP3A5-selective activity in human liver microsomes

Measurement of CYP3A and CYP3A5-selective activity: Midazolam 1´-hydroxylation was used as a marker of CYP3A activity, as described previously (Walsky and Obach, 2004). Briefly, midazolam (2.5 μM) was incubated with single-donor human liver microsomal fractions (0.03 mg protein/ml) supplemented with NADPH-regenerating system. Reactions were initiated with the addition of NADPH solution A; the final incubation volume was 0.2 ml. Control incubations were without NADPH-regenerating system. Incubations were carried out for 4 minutes at 37°C in a shaking water-bath. Reactions were quenched by the addition of 0.4 ml of ice-cold acetonitrile containing 0.1

μM d_4-1´-hydroxymidazolam (internal standard), mixed with a vortex device for 10 seconds, and centrifuged for 20 minutes at 3700 x g (4°C). The clear supernatant was transferred into LC-MS vials, and a 10 μl-aliquot was subjected to LC-MS/MS analysis. Levels of 1´-hydroxymidazolam were measured by LC-MS/MS using a standard curve (1, 5, 10, 25, 50, 100, 250, 500, 1000 nM 1´-hydroxymidazolam) (Walsky and Obach, 2004).

T-5 *N*-oxidation was used as a selective marker reaction for CYP3A5 activity, as described by Li et al. (Li et al., 2014). Briefly, T-5 (5 μM) was incubated with single-donor human liver microsomal fractions (0.1 mg protein/ml) supplemented with NADPH-generating system. Reactions were initiated with the addition of NADPH solution A; the final incubation volume was 0.2 ml. Control incubations were without NADPH-regenerating system. The final organic solvent concentration was 0.1% DMSO/ 0.9% acetonitrile (v/v). Incubations were carried out for 15 minutes at 37°C in a shaking water-bath. Reactions were quenched by the addition of 0.4 ml of ice-cold acetonitrile containing 0.1 μM d_4-1´-hydroxymidazolam (internal standard) and prepared for LC-MS analysis as described above. T-5 *N*-oxide was quantified by LC-MS/MS analysis using a standard curve (5, 10, 25, 50, 100, 250, 500, 2500 nM T-5 *N*-oxide) (Li et al., 2014). Standards were prepared in a similar matrix as the experimental samples. Working solutions of standards were diluted into 100 mM potassium phosphate, 0.1 mg protein/ml of pooled human liver microsomes without NADPH-regenerating system. For measurement of midazolam 1´-hydroxylation and T-5 *N*-oxidation, three independent experiments were performed in triplicate each.

Lapatinib metabolism in genotyped human liver microsomes

Lapatinib (5 μM) was incubated with single-donor human liver microsomal fractions (0.1 mg protein/ml) supplemented with 5 mM GSH and an NADPH-regenerating system. Reactions were initiated with the addition of NADPH solution A; the final incubation volume was 0.2 ml. Control incubations were without NADPH-regenerating system. Incubations were carried out for 20 minutes at 37°C in a shaking water-bath. Reactions were quenched by the addition of 0.4 ml of ice-cold acetonitrile containing 100 ng/ml d_4-debenzylated lapatinib (internal standard), mixed with a vortex device for 10 seconds, and centrifuged for 20 minutes at 3700 x g (4°C). The clear supernatant (~0.5 ml) was transferred to a separate vial, and the solvent was evaporated under N_2 gas using a TurboVap (Biotage; Charlotte, NC) to concentrate the samples. The dried sample residue was re-dissolved with 0.1 ml of 80:20 LC-MS-grade water/acetonitrile (v/v), mixed with a vortex device for 10 seconds, and centrifuged for 5 minutes at 20,000 x g (room temperature). The supernatant (~0.1 ml) was transferred to an LC-MS vial, and a 15-μl aliquot was subjected to LC-MS/MS analysis for measurement of relative levels of debenzylated lapatinib (M1) and quinoneimine-GSH conjugates (Hardy et al., 2014; Towles et al., 2016).

Effect of CYP3A inhibitors on lapatinib metabolism in genotyped human liver microsomes

Lapatinib (5 μM) was incubated with pooled and individual genotyped human liver microsomes (0.1 mg/ml) in 100 mM potassium phosphate buffer (pH 7.4) supplemented with 5 mM GSH and NADPH-regenerating system for 20 minutes in the

presence and absence of CYP3A4-selective inhibitor CYP3cide (2 μM) and pan-CYP3A inhibitor ketoconazole (1 μM) to determine the relative CYP3A5 contributions to lapatinib metabolite formation (Walsky et al., 2012). CYP3cide was used without pre-incubation, as described by (Tseng et al., 2014). Vehicle control incubations included solvent (1:9 DMSO: acetonitrile, v/v) without inhibitor. Reactions were initiated by the addition of NADPH solution A. Samples were processed as described above. Lapatinib metabolites were analyzed by LC-MS/MS, and metabolite formation was compared to vehicle control incubations without inhibitors. Pooled human liver microsomes from 150 donors, mixed gender (Corning Life Sciences) were used to assess metabolite formation in an "average" population. Human liver microsomes from seven individual genotyped donors were used in these experiments as follows: *CYP3A5*1/*1*, n = 4: HH860(F), HH867(M), HH785(M), 710272(F); *CYP3A5*3/*3*, n = 3: 710252(M), 719253(M), 710237(M). Two independent experiments were performed in triplicate each to assess reproducibility.

Formation of lapatinib M1 (debenzylated lapatinib) was quantified by LC-MS/MS analysis using a standard curve of chemically synthesized M1. Stock solutions of lapatinib M1 were prepared in DMSO. Working solutions were prepared in a similar matrix as the experimental samples. For quantitation from microsomal incubations, M1 standards were diluted 1:100 into 100 mM potassium phosphate, 0.1 mg protein/ml of pooled human liver microsomes without NADPH-regenerating system. Final standard concentrations of M1 were: 0.001 0.0025, 0.005, 0.01, 0.025, 0.05, 0.1, 0.25, 0.5, 1 μg/ml. M1 standards were prepared in duplicate and were analyzed by LC-MS/MS analysis with the experimental samples.

Lapatinib metabolism in genotyped human hepatocytes

Incubations with cryopreserved human hepatocytes were carried out according to the suppliers' protocols (BioIVT and Xenotech) with slight modifications. Cell viability was determined by the trypan blue exclusion method.

Lapatinib (10 μM) was incubated with pooled and single-donor cryopreserved human hepatocytes in suspension. Cells were seeded at a density of 0.5 x 10^6 cells/ml in KHB in a 24-well collagen coated-plated. The final incubation volume was 0.5 ml, and the final organic solvent concentration was 1% (1:9 DMSO/acetonitrile, v/v). Incubations with pooled-donor hepatocytes were carried out for 2 hours, and incubations with single-donor *CYP3A5*-genotyped hepatocytes were carried out for 2.2 hours in a temperature-controlled plate shaker at 37°C. To distinguish the CYP3A4 and CYP3A5 contributions to lapatinib metabolism, single-donor hepatocytes were co-incubated with the CYP3A inhibitor ketoconazole (1 μM) or the CYP3A4-selective inactivator CYP3cide (2 μM) (Walsky et al., 2012; Tseng et al., 2014). After the incubation period, sample plates were placed on ice, and an equal volume (0.5 ml) of ice-cold acetonitrile containing 100 ng/ml d_4-debenzylated lapatinib (internal standard) was added to precipitate the protein. The cell media mixture was transferred to a clean microcentrifuge tube and centrifuged for 20 minutes at 3700 x g (4°C). The clear supernatant (~0.8 ml) was transferred to a separate vial, and the solvent was evaporated under N_2 gas using a TurboVap system to concentrate the samples. Each dried sample residue was re-dissolved with 0.2 ml of 80:20 LC-MS-grade water/acetonitrile (v/v), mixed with a vortex device for 10 seconds,

and centrifuged for 5 minutes at 20,000 x g (room temperature). The supernatant (~0.2 ml) was transferred to a clean LC-MS vial, and a 15-μl aliquot was subjected to LC-MS/MS analysis for measurement of relative levels of lapatinib metabolites (Hardy et al., 2014). For quantitation of lapatinib M1 from hepatocyte incubations, M1 standard stock solutions were diluted 1:100 into KHB without cells. Final standard concentrations of M1 were: 0.001 0.0025, 0.005, 0.01, 0.025, 0.05, 0.1, 0.25, 0.5, 1 μg/ml. As noted above, M1 standards were prepared in duplicate and were analyzed by LC-MS/MS with the experimental samples.

CYP3A and CYP3A5-selective activities were measured in hepatocytes using midazolam and T-5 as probe substrates, respectively. Midazolam (2.5 μM) and T-5 (5 μM) were incubated separately with pooled and single-donor cryopreserved human hepatocytes in suspension at a cell density of 0.5 x 10^6 cells/ml in KHB in a 24-well collagen coated-plate. The final incubation volume was 0.5 ml, and the final organic solvent concentration was 1% (1:9 DMSO/acetonitrile, v/v). Incubations were carried out for 30 minutes, in a temperature-controlled plate shaker at 37°C. After the incubation period, sample plates were placed on ice, and an equal volume (0.5 ml) of ice-cold acetonitrile containing 0.1 μM d_4-1´-hydroxymidazolam (internal standard) was added. The cell media mixture was transferred to a clean microcentrifuge tube as described above and centrifuged for 20 minutes at 3700 x g (4°C). The supernatant was transferred to an LC-MS vial, and samples were subjected to LC-MS/MS analysis for measurement of 1´-hydroxymidazolam and T-5 *N*-oxide. Incubations with single-donor cryopreserved hepatocytes were performed as a single experiment on multiple days (3-

4 donors per day, for 4 days) in at least three replicates per donor. All samples were analyzed by LC-MS on the same day. Formation of 1´-hydroxymidazolam and T-5 *N*-oxide was quantified by LC-MS/MS analysis using standard curves for each compound, and levels are reported as pmol per minute per million live cells (Li et al., 2014). A standard curve of 1´-hydroxymidazolam (1, 5, 10, 25, 50, 100, 250, 500, 1000 nM) was used for quantitation of 1´-hydroxymidazolam (Walsky and Obach, 2004), and a standard curve of T-5 *N*-oxide (5, 10, 25, 50, 100, 250, 500, 2500 nM) was used for quantitation of T-5 *N*-oxide (Li et al., 2014). D_4-1´-hydroxymidazolam (0.1 μM) used as the internal standard for both analytes. Standards were prepared in a similar matrix as the experimental samples, but without cells; standards were diluted into KHB to the desired concentration. The standards were analyzed with experimental samples from incubations with cryopreserved human hepatocytes for metabolite quantitation on the same day.

Lapatinib metabolism in pooled human liver S9 fraction

Dick (Dick, 2018) recently proposed that aldehyde oxidase (AO) mediates hydroxylation of lapatinib to “AO-M1” and hydroxylation of debenzylated lapatinib to M3. To examine lapatinib metabolism by P450 and AO, lapatinib and debenzylated lapatinib (10 μM) were incubated with 10-donor pooled human liver S9 fraction (2.5 mg protein/ml) in 100 mM potassium phosphate (pH 7.4) supplemented with 5 mM GSH in the presence and absence of NADPH-generating system. The final incubation volume was 0.2 ml. Aliquots (0.08 ml) of the reaction mixture were removed at 60 and 120 minutes and combined with twice the volume (0.16 ml) of ice-cold acetonitrile containing

100 ng/ml d_4-debenzylated lapatinib (internal standard). The resulting samples were mixed with a vortex device for 10 seconds and centrifuged for 20 minutes at 20,000 x g (4°C). The clear supernatant (~0.2 ml) was transferred to a separate vial, dried under N_2 gas, and re-dissolved with 0.1 ml of 80:20 LC-MS-grade water/acetonitrile (v/v), as described above. The resulting sample was subjected to LC-MS/MS analysis for measurement of relative levels of lapatinib metabolites, including debenzylated lapatinib (M1), AO-M1 (Dick, 2018), M3 (Castellino et al., 2012), and quinoneimine-GSH conjugates (Hardy et al., 2014; Towles et al., 2016).

Lapatinib and debenzylated lapatinib metabolism in pooled human liver S9 with AO and XO inhibitors

To confirm the role of AO in the formation of lapatinib "AO-M1" and M3, and to evaluate a potential role of the related cytosolic enzyme xanthine oxidase (XO) in the formation of these metabolites, each substrate (lapatinib, 5 μM, debenzylated lapatinib, 2.5 μM) was incubated at 37°C in a potassium phosphate (100 mM, pH 7.4) buffered mixture containing 20-donor pooled human liver S9 fraction (2.5 mg protein/ml) in the presence and absence of either the AO inhibitor hydralazine (25 μM) or the XO inhibitor allopurinol (100 μM). The final incubation volume was 0.2 ml. Mixtures were pre-incubated with hydralazine (or vehicle) for 30 minutes at 37°C, and then allopurinol (or vehicle) was added to the appropriate vials immediately followed by the addition of substrate to initiate the reaction. After incubation for 60 minutes, the reaction was terminated with the addition of 0.4 ml of ice-cold acetonitrile containing 100 ng/ml d_4-debenzylated lapatinib (internal standard). The resulting samples were centrifuged for

20 minutes at 3740 x g (4°C). The clear supernatant (0.2 ml) was transferred to a separate vial for LC-MS/MS analysis of AO-M1 or M3 formation. Two independent experiments were performed in triplicate to verify reproducibility, and an incubation with heat inactivated S9 (pre-heated at ~100°C for 10 minutes) was included to serve as a negative control. No positive control for XO activity was included; however, the S9 fractions were previously characterized for both AO and XO activity by the vendor (XenoTech), confirming active AO and XO. Some human liver S9 and/or cytosolic fractions have been reported to lack XO activity due to the use of allopurinol during liver tissue processing (Barr et al., 2014). However, according to the vendor, human liver S9 fractions used in these studies were processed in the absence of allopurinol. Positive control incubations with the known AO substrate O^6-benzylguanine (5 μM) were included to confirm AO activity (Roy et al., 1995). AO activity was confirmed by monitoring 8-oxidation of O^6-benzylguanine (8-oxo-benzylguanine formation) in positive control incubations (data not shown).

LC-MS/MS analysis of metabolites

Metabolites of lapatinib and probe substrates were measured by LC-MS/MS analysis. The LC-MS/MS system was similar to that described by (Amaya et al., 2018). Briefly, a Shimadzu Prominence XR UHPLC system was equipped with two Shimadzu LC-20ADXR pumps, a SIL-20ACXR autosampler, and a CTO-20A column oven heated to 32 °C. The UHPLC system was coupled to a Shimadzu MS/MS 8030 triple quadrupole mass spectrometer (Amaya et al., 2018). A Phenomenex Kinetex C18 octadecylsilane column (2.6 mm, 50 x 2.1 μm, 100 Å) was used to achieve analyte

separation. The mobile phase flow rate was 0.3 ml/min. Mobile phase A was 0.1% formic acid in LC-MS-grade water, and mobile phase B was 0.1% formic acid in LC-MS-grade acetonitrile (v/v). Two UHPLC gradient programs were used for analysis of lapatinib metabolites and marker reactions. LC gradient program 1 was as follows: 0 – 1.0 min (5% B), linear gradient from 1.0 – 2.0 min (5 to 95% B), 2.0 – 3.5 min (95% B), 3.5 – 3.6 min (95 to 5% B), 3.6 – 5 min (5% B) (all v/v). LC gradient program 2, which was used for quantitation of lapatinib M1, was as follows: linear gradient from 0 – 2.00 min (10 to 95% B), 2.00 – 2.50 min (95% B), 2.50 – 2.51 min (95 to 10% B), 2.51 – 4.00 min (10% B) (all v/v). A sample injection volume of 10-15 μl was injected via an autosampler onto an equilibrated UHPLC column, and the eluent was introduced directly into the mass spectrometer via electrospray ionization (ESI) in positive ion mode. MS spectral data were acquired and analyzed using Shimadzu LabSolutions software (Amaya et al., 2018).

Lapatinib, probe substrates, and their respective metabolites were detected and quantified by LC-MS/MS utilizing multiple reaction monitoring (MRM). The MRM precursor-to-product ion transitions for lapatinib and lapatinib metabolites were: *m/z* 581.6 → 365 (lapatinib), *m/z* 473 → 350 (debenzylated lapatinib, M1), *m/z* 778 → 655 (quinoneimine-GSH conjugate), as described previously (Towles et al., 2016). The MRM transitions for the putative AO-mediated metabolites of lapatinib and debenzylated lapatinib were: *m/z* 597 → 474 (AO-M1), *m/z* 489 → 366 (M3) (Castellino et al., 2012; Dick, 2018). Formation of 1´-hydroxymidazolam (measure of CYP3A activity) was detected using the MRM transition *m/z* 342 → 324, and d_4-1´-hydroxymidazolam (*m/z* 346 → 328) was used as the internal standard, according to the methods described by

(Walsky and Obach, 2004). The MRM transitions for T-5 and T-5 metabolites were: *m/z* 568.2 → 476.2 (T-5), *m/z* 584.2 → 476.2 (T-5 *N*-oxide), *m/z* 477.2 → 445.2 (*O*-dealkylated T-5), according to the methods described previously (Li et al., 2014).

Formation of 8-oxo-benzylguanine (from O^6-benzylguanine) was determined employing LC-MS/MS analysis with an electrospray ionization enabled Sciex QTRAP 6500 triple quadrupole instrument (Sciex, Foster City, CA) that was coupled to Shimadzu LC-20ADXR pumps (Shimadzu, Columbia, MD) and a CTC PAL autosampler (Leap Technologies, Carrboro, NC). Analytes were separated by gradient elution following a 10 μl injection onto a Phenomenex Kinetex EVO C18 100 Å column (1.7 μm, 50 x 2.1 mm) operating at 40°C. Mobile phase A was 0.1% formic acid in LC-MS grade water and mobile phase B was 0.1% formic acid in LC-MS grade acetonitrile (v/v). The flow rate was 0.5 ml/min, and the LC gradient was as follows: 0 - 0.2 min (5% B), linear gradient from 0.2 – 1.2 min (5 - 95% B), 1.2 – 1.4 min (95% B), 1.4 – 1.5 min (95 – 5% B), 1.5 – 2.0 min (5% B). The total run time was 2.0 min. Mass spectral analyses were performed using multiple reaction monitoring (MRM), with transitions and voltages specific for each analyte, using a Turbo Ion Spray source (source temp 650°C) in positive ionization mode (5.5 kV spray voltage). MRM transitions were the following: O^6-benzylguanine (*m/z* 242→199), 8-oxo-benzylguanine (*m/z* 258→91) (Barr et al., 2014), and the internal standard, carbamazepine (*m/z* 237→194). Data were analyzed using Sciex Analyst 1.7.0 software.

Statistical Analysis

All statistical analyses were performed using GraphPad Prism 7 software (GraphPad, San Diego, CA). Formation of lapatinib M1 and quinoneimine-GSH conjugates in single-donor human liver microsomes and hepatocytes was analyzed for correlation with midazolam 1´-hydroxylation (CYP3A activity) and T-5 *N*-oxidation (CYP3A5-selective activity) using linear regression analysis and Pearson *r* correlation. Lapatinib metabolism, midazolam 1´-hydroxylation, and T-5 *N*-oxidation were compared across *CYP3A5* genotypes (**1/*1, *1/*3,* and **3/*3*) by one-way ANOVA. Comparison of lapatinib M1 formation and midazolam 1´-hydroxylation by sex (male vs. female) was performed by unpaired student t-test. Outlier analysis was conducted using Grubb's outlier method. Experiments were performed in triplicate unless otherwise stated. Statistical significance was determined at $p < 0.05$.

DMD Fast Forward. Published on September 6, 2019 as DOI: 10.1124/dmd.119.088823
This article has not been copyedited and formatted. The final version may differ from this version.

Results

Measurement of CYP3A and CYP3A5 activity in genotyped human liver microsomes

CYP3A and CYP3A5-selective activity were measured in *CYP3A5*-genotyped human liver microsomes to assess the genotype-phenotype relationship. Individual human liver microsomal samples included: *CYP3A5*3/*3* donors, n = 5; *CYP3A5*1/*3* donors, n = 3; *CYP3A5*1/*1* donors, n = 4. CYP3A activity, as measured by midazolam 1´-hydroxylation, varied widely between liver microsomes from individual donors (23 to 1754 pmol/min/mg protein). However, midazolam 1´-hydroxylation did not significantly differ when compared by *CYP3A5* genotype among the 12 donors analyzed in this study (one-way ANOVA, P = 0.2775) (Figure 1A).

T-5 *N*-oxidation has been reported as a selective marker reaction for CYP3A5 activity (Li et al., 2014). In the present study, T-5 *N*-oxide formation in human liver microsomes was significantly associated with *CYP3A5* genotype in the following order: *CYP3A5 *3/*3* < **1/*3* < **1/*1* (one-way ANOVA, P < 0.0001) (Figure 1B). The rates of T-5 *N*-oxidation in human liver microsomal samples were 0 to 2.1 pmol/min/mg protein among *CYP3A5*3/*3* donors (n = 5); 3.4 to 9.0 pmol/min/mg protein in *CYP3A5*1/*3* donors (n = 3); and 12 to 25 pmol/min/mg protein in *CYP3A5*1/*1* donors (n = 4). Moreover, the mean rates of T-5 *N*-oxide formation were 19-fold higher in *CYP3A5*1/*1* donors compared to *CYP3A5*3/*3* donors (mean ± SD): 19 ± 5.3 vs. 1.0 ± 0.9 pmol/min/mg protein, respectively. These results confirm the positive relationship

between *CYP3A5* genotype and CYP3A5 enzyme activity in human liver microsomal fractions.

Lapatinib bioactivation in genotyped human liver microsomes

Formation of debenzylated lapatinib (M1) and quinoneimine-GSH conjugates was examined in *CYP3A5*-genotyped human liver microsomes from 11 of the 12 donors analyzed above. (*CYP3A5*1/*3* donor HH757 was not included in this analysis due to the limited amount of this sample available at the time of analysis). Relative levels of M1 (peak area ratio) trended toward higher formation in *CYP3A5*1/*1* donors compared to *CYP3A5*3/*3* donors, but the difference was not statistically significant (Figure 2A). Relative levels of quinoneimine-GSH conjugates did not differ by *CYP3A5* genotype in human liver microsomes (Figure 2B).

M1 formation was significantly correlated with CYP3A activity, as measured by midazolam 1´-hydroxylation (r^2 = 0.75, n = 11, P = 0.0006), and CYP3A5-selective activity, as measured by T-5 *N*-oxidation (r^2 = 0.51, n = 11, P = 0.0142) in human liver microsomes (Figure 3A-B). Formation of quinoneimine-GSH conjugates was significantly correlated with midazolam 1´-hydroxylation (r^2 = 0.91, n = 11, P < 0.0001), but not T-5 *N*-oxidation (r^2 = 0.32, n = 11, P = 0.0681) (Figure 3C-D). The relationship between lapatinib *O*-debenzylation and subsequent quinoneimine formation was also evaluated. Formation of quinoneimine-GSH conjugates significantly correlated with the levels of M1 (r^2 = 0.83, n = 11, P < 0.0001) (Figure 3E). This is consistent with the fact that debenzylated lapatinib (M1) is a precursor to the reactive quinoneimine (Teng et al., 2010). Collectively, these results demonstrate that lapatinib bioactivation via oxidative

O-debenzylation and formation of the reactive quinoneimine (trapped as a GSH conjugate) is strongly correlated with total microsomal CYP3A activity (midazolam 1´-hydroxylation).

Effect of CYP3A-selective inhibitors on microsomal lapatinib *O*-debenzylation

Recently developed CYP3A4-selective inhibitors have allowed for distinguishing CYP3A4 vs. CYP3A5 contributions to drug metabolism *in vitro* (Walsky et al., 2012). We examined the relative contributions of CYP3A4 and CYP3A5 to lapatinib *O*-debenzylation in human liver microsomes using the CYP3A4-selective inactivator CYP3cide and pan-CYP3A inhibitor ketoconazole. Human liver microsomes from single donors genotyped as *CYP3A5*1/*1* (n = 4) and *CYP3A5*3/*3* (n = 3) were used for this analysis. The difference in percent inhibition by CYP3cide (CYP3A4-selective inhibitor) vs. ketoconazole (pan-CYP3A inhibitor) was used to estimate CYP3A5 contribution to microsomal M1 formation. The results from this analysis are shown graphically in Figure 4 and are summarized in Table 1. Notably, the average rate of M1 formation was similar between *CYP3A5*3/*3* donors (50 ± 33 pmol/min/mg protein, n = 3) and pooled human liver microsomes from 150 donors (50 pmol/min/mg protein); whereas, the average rate of M1 formation was slightly higher among *CYP3A5*1/*1* donors (65 ± 29 pmol/min/mg protein, n = 4).

In human liver microsomes from *CYP3A5*1/*1* donors (n = 4), coincubation with CYP3cide (2 μM) reduced M1 formation by 62 ± 7% (mean ± SD), compared to control incubations without inhibitor; ketoconazole reduced M1 levels by 88 ± 3 %, compared to control incubations. The estimated average CYP3A5 percent contribution among

*CYP3A5*1/*1* donors was 26 ± 5% (range 20 – 31 %). For *CYP3A5*3/*3* human liver microsomes (n = 3), coincubation with CYP3cide decreased M1 formation by 84 ± 2 % compared to control levels, and ketoconazole reduced debenzylated lapatinib generation by 92 ± 1 %, compared to control incubations. The estimated residual CYP3A5 contribution among *CYP3A5*3/*3* donors was 8 ± 2 % (range 6 – 10%). Collectively, these results demonstrate that the CYP3A5 contribution to lapatinib *O*-debenzylation was significantly higher in CYP3A5 expressers (*CYP3A5*1/*1*) compared to *CYP3A5*3/*3* donors: 26 ± 5 % vs. 8 ± 2 % ($p = 0.0022$). The CYP3A5 contribution to M1 formation in 150-donor pooled human liver microsomes was estimated to be 16% (Table 1).

Interestingly, the estimated CYP3A5 percent contribution to lapatinib M1 formation was positively correlated with microsomal CYP3A5 activity, as measured by T-5 *N*-oxidation, in the small subset of liver microsomal samples tested ($r^2 = 0.87$; $n = 7$) (Supplemental Figure S1). Higher liver microsomal CYP3A5 activity was associated with higher relative CYP3A5 involvement in lapatinib M1 formation.

Lapatinib metabolism in genotyped human hepatocytes from pooled donors

CYP3A activity and lapatinib metabolism were also examined in cryopreserved human hepatocytes from *CYP3A5*-genotyped donors. An initial test was conducted with *CYP3A5*-genotyped hepatocytes pooled from three donors per genotype to evaluate the relationship between CYP3A activity and lapatinib bioactivation in intact cells. Midazolam 1´-hydroxylation was 1.7 to 2.1-fold higher in pooled human hepatocytes from *CYP3A5*1/*1* and *CYP3A5*1/*3* donors (18 and 22 pmol/min/million cells),

respectively, compared to *CYP3A5*3/*3* donors (10 pmol/min/million cells) (Figure 5A). T-5 *N*-oxidation, was 6.5 – 8.6-fold higher in pooled hepatocytes from *CYP3A5*1/*1* and *CYP3A5*1/*3* donors (4.4 and 5.8 pmol/min/million cells), respectively, compared to non-expressers (*CYP3A5*3/*3*, 0.67 pmol/min/million cells) (Figure 5B). Relative levels of lapatinib M1 formation were 2.4-fold higher in pooled hepatocytes from *CYP3A5*1/*1* and *CYP3A5*1/*3* donors (CYP3A5 expressers) compared to *CYP3A5*3/*3* donors (Figure 5C). In this analysis, quinoneimine-GSH conjugates were only detectable in hepatocyte incubations from *CYP3A5*1/*1* and *CYP3A5*1/*3* donors, which had relatively high CYP3A activity. Quinoneimine-GSH conjugates were not detectable in hepatocytes from *CYP3A5*3/*3* donors (data not shown).

Lapatinib metabolism in genotyped human hepatocytes from single donors

To further investigate individual variability in CYP3A activity and lapatinib metabolism, we performed a series of experiments with cryopreserved human hepatocytes from fifteen individual *CYP3A5*-genotyped donors: *CYP3A5*3/*3* donors, n = 8; *CYP3A5*1/*3* donors, n = 5; *CYP3A5*1/*1* donors, n = 2. Donor demographic information provided by BioIVT is presented in Supplemental Table S1. Midazolam 1´-hydroxylation, a measure of CYP3A activity, varied 37-fold between all donors (1.5 to 54 pmol/min/million cells), but did not differ by *CYP3A5* genotype (Figure 6A). *CYP3A5*3/*3* donor JYS (female, Pacific Islander) had the highest rate of 1´-hydroxymidazolam formation (54 pmol/min/million cells). Of note, donor JYS was identified as an outlier among *CYP3A5*3/*3* donors with respect to midazolam 1´-hydroxylation based on Grubbs (α= 0.05) outlier identification method (GraphPad Prism

7). Among CYP3A5 expressers, donors RQM (*CYP3A5*1/*1*, female, African-American) and OWY (*CYP3A5*1/*3*, female, Caucasian), had relatively high rates of midazolam 1´-hydroxylation at 45 and 42 pmol/min/million cells, respectively. Rates of the CYP3A5-selective marker reaction, T-5 *N*-oxidation, were significantly higher in human hepatocyte incubations from *CYP3A5*1/*1* (9.4 ± 1.5 pmol/min/million cells, n = 2) and *CYP3A5*1/*3* donors (16.4 ± 9.3 pmol/min/million cells, n = 5), compared to *CYP3A5*3/*3* donors (1.7 ± 0.7 pmol/min/million cells, n = 8 (one-way ANOVA, P = 0.0017) (Figure 6B).

Lapatinib metabolism was examined in this same set of genotyped human hepatocytes. Rates of debenzylated lapatinib (M1) formation, varied 39-fold among individual hepatocyte donors (range 0.05 to 2.1 pmol/min/million cells, n = 15). Mean rates of midazolam 1´-hydroxylation were 2-fold higher in females compared to males (27 ± 19 vs. 12 ± 7 pmol/min/million cells, females n = 7, males n = 8, respectively), but this difference was not statistically significant (P = 0.0541). Donor JYS had the highest M1 formation (2.1 pmol/min/million cells). In comparison by *CYP3A5* genotype, JYS was identified as an outlier among *CYP3A5*3/*3* donors with respect to M1 formation. When JYS was excluded from this analysis as an outlier, the mean M1 formation was greater than 2-fold higher in *CYP3A5*1/*1* (0.73 ± 0.43 pmol/min/million cells, n = 2) and *CYP3A5*1/*3* donors (0.66 ± 0.39 pmol/min/million cells, n = 5) compared to *CYP3A5*3/*3* donors (0.29 ± 0.18 pmol/min/million cells, n = 7); however, when JYS was included in the analysis, mean M1 formation among *CYP3A5*3/*3* donors was 0.5 ± 0.6 pmol/min/million cells (n = 8). There was no statistically significant difference in M1 formation based on *CYP3A5* genotype (Figure 7). When compared by sex, M1

formation was 2.6-fold higher in females (0.88 pmol/min/million cells, n = 7) compared to males (0.34 pmol/min/million cells, n = 8) (P = 0.0442) (Supplemental Figure S3A).

Notably, formation of lapatinib M1 was strongly correlated with midazolam 1´-hydroxylation (CYP3A activity) in human hepatocytes among all donors tested (r^2 = 0.87, P < 0.0001, n = 15) (Figure 8A). M1 formation was not correlated with T-5 *N*-oxidation in this set of hepatocyte donors (r^2 = 0.07, P = 0.3578, n = 15) (Figure 8B).

Formation of quinoneimine-GSH conjugates from lapatinib was also examined in *CYP3A5*-genotyped single-donor human hepatocytes. Quinoneimine-GSH conjugates were detectable from incubations with eight of the 15 individual donors (Supplemental Figure S2B). This result may be due to the limited sensitivity of our LC-MS/MS method to detect reactive metabolite-GSH conjugates generated in intact hepatocytes from lapatinib at a substrate concentration of 10 μM. Among the samples with detectable quinoneimine-GSH conjugates, the relative levels varied among individual donors (0.001 to 0.04 peak area ratio, n = 8). Similar to lapatinib M1, quinoneimine-GSH conjugate formation was significantly correlated with CYP3A activity, as measured by midazolam 1´-hydroxylation (r^2 = 0.76, P = 0.0045, n = 8) (Figure 9A). However, quinoneimine-GSH conjugate formation was not correlated with CYP3A5-selective activity, as measured by T-5 *N*-oxidation (r^2 = 0.06, P = 0.5678, n = 8) (Figure 9B). Among the hepatocyte donors tested, donor JYS (*CYP3A5*3/*3*) had the highest levels of M1 and quinoneimine-GSH conjugates as well as the highest CYP3A activity (formation of 1´-hydroxymidazolam).

Effect of CYP3A and CYP3A4-selective inhibition on lapatinib metabolism in genotyped hepatocytes

Selective CYP3A chemical inhibitors were also used to estimate the contributions of CYP3A4 and CYP3A5 to lapatinib *O*-debenzylation in human hepatocytes from *CYP3A5*-genotyped donors. Two donors with the highest relative levels of lapatinib M1 formation were selected for comparison based on genotype and enzyme activity: JYS and OWY. Donor JYS (*CYP3A5*3/*3*) had low CYP3A5 activity, as indicated by the rate of T-5 *N*-oxidation (selective marker of CYP3A5 activity) at 3.0 pmol/min/million cells. Donor OWY (*CYP3A5*1/*3*) had relatively high CYP3A5 activity, as indicated by a rate of T-5 *N*-oxidation at 19.5 pmol/min/million cells (Figure 6B). As noted above, total CYP3A activity, measured by midazolam 1´-hydroxylation, was similar between donors JYS and OWY (54 and 42 pmol/min/million cells, respectively) (Figure 6A). In hepatocyte incubations from JYS (CYP3A5 “non-expresser”), co-incubation with the CYP3A4-selective inactivator CYP3cide reduced lapatinib M1 formation by 94%, compared to vehicle control. The pan-CYP3A inhibitor ketoconazole reduced M1 formation by 95% (Figure 10A), indicating that lapatinib M1 formation was predominantly mediated by CYP3A4. In hepatocyte incubations with OWY (CYP3A5 expresser), CYP3cide decreased levels of M1 by 45%, while ketoconazole reduced M1 levels by 87%, compared to vehicle control (Figure 10B). This finding suggests that the remaining hepatic CYP3A5 activity contributed 42% to lapatinib M1 formation in CYP3A5 expresser OWY.

Additional metabolites of lapatinib

We also examined lapatinib metabolism via non-P450 pathways as potentially competing routes of biotransformation in primary human hepatocytes. The hydroxylated metabolite of lapatinib ("AO-M1"), proposed by Dick (Dick, 2018), and hydroxylated debenzylated lapatinib (M3) were observed in hepatocyte incubations. Relative levels of AO-M1 did not differ between CYP3A5 expressers and non-expressers. An inverse relationship was observed between formation of debenzylated lapatinib (M1) and AO-M1 in human hepatocytes from individual donors ($r = -0.62$; $r^2 = 0.38$, $P = 0.0145$) (Supplemental Figure S4). To confirm the role of AO in generating the hydroxylated metabolite of lapatinib ("AO-M1") and the hydroxylated metabolite of debenzylated lapatinib M3, we conducted experiments with human liver S9 fraction, which contains both microsomal and cytosolic enzymes. Pre-incubation with the AO inhibitor hydralazine (25 μM) reduced formation of AO-M1 from lapatinib by 99% compared to control incubations without inhibitor. Hydralazine also reduced M3 formation from debenzylated lapatinib by 92%, compared to control. The xanthine oxidase inhibitor (and AO substrate) allopurinol (100 μM) decreased AO-M1 formation by 27%, compared to control, and had a minimal effect on M3. These data demonstrate that AO catalyzes the oxidation of lapatinib and debenzylated lapatinib to AO-M1 and M3, respectively (Figure 11 and Supplemental Figure S5).

Discussion

CYP3A4 and CYP3A5 are the primary enzymes responsible for oxidative metabolism of lapatinib via *O*-debenzylation, leading to formation of an electrophilic quinoneimine; this pathway has been implicated in the development of lapatinib-induced liver injury (Teng et al., 2010; Takakusa et al., 2011; Castellino et al., 2012). We hypothesized that *CYP3A5* genotype would have a significant impact on the generation of reactive metabolites from lapatinib. However, the findings of the present study indicate that lapatinib bioactivation is highly correlated with total hepatic CYP3A activity, and not *CYP3A5* genotype alone. Formation of debenzylated lapatinib (M1) was significantly correlated with CYP3A activity (midazolam 1´-hydroxylation) in human liver microsomes (r^2 = 0.75) (Figure 3) and primary human hepatocytes (r^2 = 0.87) (Figure 8). Relative levels of quinoneimine-GSH conjugates were also strongly correlated with midazolam 1´-hydroxylation in human liver microsomes (r^2 = 0.91) (Figure 3) and human hepatocytes (r^2 = 0.76) (Figure 9).

Wide inter-individual variation in CYP3A activity was observed in this study; midazolam 1´-hydroxylation varied 76-fold and 37-fold in human liver microsomes and primary human hepatocytes, respectively, which is consistent with previous reports. Moreover, lapatinib *O*-debenzylation varied 7-fold in individual human liver microsomes and 39-fold in primary human hepatocytes from individual donors. Lin et al. (2002) reported 68-fold variation in total hepatic CYP3A protein content in human liver microsomes from 60 Caucasian donors, and midazolam 1´-hydroxylation varied 28-fold among these donors. Lambda et al. (Lamba et al., 2002) reported that CYP3A

expression can vary 40-fold in human liver and intestine. Genetic and non-genetic factors have been shown to influence CYP3A activity (Klein and Zanger, 2013; Zanger and Schwab, 2013). Variation in nuclear receptors that regulate CYP3A4 expression (e.g. pregnane X receptor, constitutive androstane receptor) are known to contribute to inter-individual variability in CYP3A activity (Lamba et al., 2010; Zanger and Schwab, 2013). Enzyme induction and inhibition, epigenetics, and disease states also influence CYP3A activity (Zanger and Schwab, 2013). Conflicting results have been reported regarding gender differences in CYP3A activity (i.e. males vs. females) (Lin et al., 2002; Yang et al., 2010; Achour et al., 2014). In the present study, females had 2-fold higher CYP3A activity (midazolam 1´-hydroxylation) compared to males in hepatocyte incubations, but this was not statistically significant (P = 0.0541). Hepatocytes from female donors formed 2.6-fold higher levels of lapatinib M1 compared to males (P = 0.0442).

The CYP3A5-selective marker reaction T-5 *N*-oxidation, described by Li et al. (2014), was used to characterize CYP3A5 activity in *CYP3A5*-genotyped human liver microsomal samples and cryopreserved human hepatocytes. T-5 *N*-oxidation was significantly associated with the *CYP3A5* genotype in human liver microsomes (Figure 1) and in primary human hepatocytes (Figure 6), indicating a strong CYP3A5 genotype – phenotype relationship. Individual livers carrying at least one *CYP3A5*1* allele had significantly higher CYP3A5 activity compared to livers homozygous for *CYP3A5*3*. Formation of lapatinib M1 was correlated with T-5 *N*-oxidation in human liver microsomes (r^2 = 0.51) (Figure 3), but not in primary human hepatocytes (r^2 = 0.07) (Figure 8). The reason for this discrepancy between microsomes and hepatocytes is not

known and warrants further investigation. Relative levels of quinoneimine-GSH conjugates were not associated with CYP3A5 activity (T-5 *N*-oxidation) in human liver microsomes (r^2 = 0.32) (Figure 3), or primary human hepatocytes (r^2 = 0.06) (Figure 9). Formation of lapatinib M1 and quinoneimine-GSH conjugates did not significantly differ by *CYP3A5* genotype (Figure 2). These results indicate that CYP3A5 genotype and activity alone are not predictive of lapatinib bioactivation.

CYP3A4 and CYP3A5 contributions to lapatinib *O*-debenzylation were estimated in human liver microsomes and cryopreserved hepatocytes based on the percent inhibition by CYP3cide (CYP3A4-selective inactivator) compared to inhibition by ketoconazole (CYP3A-pan inhibitor), as described previously (Walsky et al., 2012; Tseng et al., 2014). The contributions of CYP3A4 vs. CYP3A5 to lapatinib *O*-debenzylation varied by individual; but, CYP3A4 played a dominant role in lapatinib metabolism in all donors. Of the total CYP3A contribution, CYP3A4 contributed greater than 90% on average to lapatinib M1 formation in *CYP3A5*3/*3* livers. The estimated CYP3A4 contribution was approximately 60-75% in livers homozygous or heterozygous for *CYP3A5*1*. CYP3A5 contributed an estimated 20 – 42% to M1 formation in livers from individuals carrying the *CYP3A5*1* allele. In addition to the *O*-debenzylation pathway, lapatinib is metabolized via *N*-hydroxylation and *N*-dealkylation predominately by CYP3A4 (Takakusa et al., 2011). Differential interactions of lapatinib with CYP3A4 and CYP3A5 can have unique effects on enzyme activity and product regioselectivity (Takakusa et al., 2011; Chan et al., 2012; Barbara et al., 2013). Lapatinib is a time-dependent inhibitor of CYP3A4 through metabolic-intermediate complex formation, which is thought to occur primarily by lapatinib *N*-hydroxylation and subsequent

oxidation to a nitroso intermediate (Takakusa et al., 2011). In contrast, inactivation of CYP3A5 by lapatinib may occur through adduction of the quinoneimine to the apoprotein (Chan et al., 2012).

To our knowledge, this is the first study to examine the effect of *CYP3A5* genotype, CYP3A5-selective activity, and total CYP3A activity on lapatinib bioactivation in individual human liver tissues from multiple donors. The dominant role of CYP3A4 in lapatinib bioactivation observed in the present study is consistent with previous studies. In kinetic analyses with recombinant CYP3A4 and CYP3A5, recombinant CYP3A4 was 5-fold more efficient at lapatinib *O*-debenzylation and 4-fold more efficient at generating quinoneimine-GSH conjugates compared to recombinant CYP3A5 (Towles et al., 2016). Inhibition studies with pooled human liver microsomes demonstrated that CYP3A5 contributed 16-22% to generating quinoneimine-GSH conjugates (Towles et al., 2016). Previous studies reported that CYP3A5 genotype may influence the levels of quinoneimine-GSH conjugates formed *in vitro* (Chan et al., 2014; Ho et al., 2015); however, these findings have not been replicated *in vivo*. As noted above, wide (39-fold) inter-individual variation in lapatinib *O*-debenzylation was observed in the present study, which was highly associated with CYP3A activity. This suggests that measuring individual CYP3A phenotype, and not *CYP3A5* genotype alone, may be an important approach to better assess individual drug metabolism status and improve precision dosing.

Lapatinib pharmacokinetics exhibit high inter-individual variability in cancer patients, and variation in CYP3A-mediated metabolism is suggested to contribute, at least in part, to differences in lapatinib exposure (Burris et al., 2005). Because CYP3A-

mediated *O*-debenzylation is a major route of lapatinib metabolism, factors that alter CYP3A expression and activity likely have a significant impact on the extent of lapatinib bioactivation. In addition, non-P450 pathways may contribute to lapatinib metabolism and variability in drug exposure. Consistent with the recent findings by Dick (Dick, 2018), we have shown that aldehyde oxidase catalyzes hydroxylation of lapatinib to AO-M1 and oxidation of lapatinib M1 to M3, a major metabolite excreted *in vivo* (Figure 11) (Castellino et al., 2012). Further, lapatinib is a substrate for efflux transporters P-glycoprotein (Pgp, ABCB1) and breast cancer resistance protein (BCRP), and lapatinib is an inhibitor of Pgp, BCRP, and organic anion transporting polypeptide 1B1 (OATP1B1) at clinically relevant concentrations (Polli et al., 2008). Lapatinib M1 was suggested to be an inhibitor of BSEP, the bile salt export pump (Castellino et al., 2012). Further research is needed to assess the role of altered drug metabolism and transport on the risk of lapatinib-induced hepatotoxicity in the clinical setting.

An association between CYP3A4 genotype, protein abundance, and/or activity, and drug exposure has been shown for other clinically relevant tyrosine kinase inhibitors. Using midazolam as a CYP3A phenotyping probe in cancer patients, Barr et al. (2014) and de Wit et al. (2014) demonstrated that sunitinib exposure was significantly correlated with midazolam exposure; intestinal and hepatic CYP3A activity was proposed to explain approximately 40-50% of the inter-patient viability in sunitinib exposure. Presence of the CYP3A4 reduced function allele **22* was shown to reduce pazopanib clearance in simulated cancer patients compared to patients with wildtype CYP3A4 (Bins et al., 2019). Moreover, using a physiologically based pharmacokinetic (PBPK) model, Sorich et al., (2019) reported that CYP3A abundance was the dominant

factor affecting variability in exposure to axitinib. Together, these studies indicate that CYP3A phenotype may have a significant influence on the pharmacokinetics of tyrosine kinase inhibitors and other classes of drugs predominately metabolized by CYP3A.

The limitations of this study include the small sample size and limited genetic information. Commercially available *CYP3A5*-genotyed human liver microsomes and cryopreserved hepatocytes are in limited supply, especially among donors expressing CYP3A5. The human liver samples included in this study were genotyped for *CYP3A5 *1* and **3* alleles, but not CYP3A5 variant alleles **6* and **7*, which also cause reduced CYP3A5 expression (Kuehl et al., 2001). Livers were not genotyped for *CYP3A4*22*, which is linked to reduced CYP3A4 mRNA levels and enzymatic activity (Wang et al., 2011; Wang and Sadee, 2016). CYP3A4 and CYP3A5 protein levels and mRNA expression were not analyzed; however, measurement of CYP3A and CYP3A5-selective activity using established probe substrates and marker reactions provided a relevant indicator of CYP3A functional status. Donor JYS was identified as an outlier among *CYP3A5*3/*3* donors with respect to CYP3A activity and lapatinib metabolism. The medical history of this and other donors is not known; thus, we do not know whether donors were taking medications or dietary supplements that alter CYP3A activity. Additional information is needed to understand why this donor (JYS) had relatively high CYP3A activity; however, such information is not available due to privacy restrictions.

In summary, the results of this study indicate that total CYP3A activity is a major determinant of the extent of lapatinib bioactivation. Inter-individual variation in lapatinib metabolic activation was highly correlated to individual CYP3A activity. Factors that

influence CYP3A activity likely affect individual exposure to reactive, potentially toxic metabolites of lapatinib. Future studies are warranted to assess the utility of CYP3A phenotyping *in vivo* to guide lapatinib dosing and predict the risk of lapatinib toxicity in clinical settings.

Acknowledgements

The authors thank Dr. Michael Cameron (Scripps Research Institute) for generously providing T-5 (T-1032) and T-5 *N*-oxide standards for CYP3A5 phenotyping studies. We also thank Dr. F. Peter Guengerich and his group (Vanderbilt University) for valuable scientific discussions during the manuscript preparation and Dr. Matthew Vergne for assistance with LC-MS/MS instrumentation in the Lipscomb University College of Pharmacy Bioanalytical Core Laboratory.

Authorship Contributions

Participated in research design: Bissada, Abouda, Wines, Crouch, and Jackson

Conducted experiments: Bissada, Truong, Abouda, Wines, Crouch, and Jackson

Contributed new reagents or analysis tools:

Performed data analysis: Bissada, Truong, Abouda, Wines, Crouch, and Jackson

Wrote or contributed to the writing of the manuscript: Bissada, Truong, Abouda, Crouch, and Jackson

References

Achour B, Barber J, and Rostami-Hodjegan A (2014) Expression of hepatic drug-metabolizing cytochrome P450 enzymes and their intercorrelations: a meta-analysis. *Drug Metab Dispos* **42:**1349-1356.

Amaya GM, Durandis R, Bourgeois DS, Perkins JA, Abouda AA, Wines KJ, Mohamud M, Starks SA, Daniels RN, and Jackson KD (2018) Cytochromes P450 1A2 and 3A4 catalyze the metabolic activation of sunitinib. *Chem Res Toxicol* **31:**570-584.

Aoyama T, Yamano S, Waxman DJ, Lapenson DP, Meyer UA, Fischer V, Tyndale R, Inaba T, Kalow W, Gelboin HV, and et al. (1989) Cytochrome P-450 hPCN3, a novel cytochrome P-450 IIIA gene product that is differentially expressed in adult human liver. cDNA and deduced amino acid sequence and distinct specificities of cDNA-expressed hPCN1 and hPCN3 for the metabolism of steroid hormones and cyclosporine. *J Biol Chem* **264:**10388-10395.

Azim HA, Jr., Agbor-Tarh D, Bradbury I, Dinh P, Baselga J, Di Cosimo S, Greger JG, Jr., Smith I, Jackisch C, Kim SB, Aktas B, Huang CS, Vuylsteke P, Hsieh RK, Dreosti L, Eidtmann H, Piccart M, and de Azambuja E (2013) Pattern of rash, diarrhea, and hepatic toxicities secondary to lapatinib and their association with age and response to neoadjuvant therapy: analysis from the NeoALTTO trial. *J Clin Oncol* **31:**4504-4511.

Barbara JE, Kazmi F, Parkinson A, and Buckley DB (2013) Metabolism-dependent inhibition of CYP3A4 by lapatinib: evidence for formation of a metabolic

intermediate complex with a nitroso/oxime metabolite formed via a nitrone intermediate. *Drug Metab Dispos* **41**:1012-1022.

Barr JT, Choughule KV, Nepal S, Wong T, Chaudhry AS, Joswig-Jones CA, Zientek M, Strom SC, Schuetz EG, Thummel KE, and Jones JP (2014) Why do most human liver cytosol preparations lack xanthine oxidase activity? *Drug Metab Dispos* **42:**695-699.

Bins S, Huitema ADR, Laven P, Bouazzaoui SE, Yu H, van Erp N, van Herpen C, Hamberg P, Gelderblom H, Steeghs N, Sleijfer S, van Schaik RHN, Mathijssen RHJ, and Koolen SLW (2019) Impact of CYP3A4*22 on pazopanib pharmacokinetics in cancer patients. *Clin Pharmacokinet* **58:**651-658.

Birdwell KA, Decker B, Barbarino JM, Peterson JF, Stein CM, Sadee W, Wang D, Vinks AA, He Y, Swen JJ, Leeder JS, van Schaik R, Thummel KE, Klein TE, Caudle KE, and MacPhee IA (2015) Clinical pharmacogenetics implementation consortium (CPIC) guidelines for CYP3A5 genotype and tacrolimus dosing. *Clin Pharmacol Ther* **98:**19-24.

Burris HA, 3rd, Hurwitz HI, Dees EC, Dowlati A, Blackwell KL, O'Neil B, Marcom PK, Ellis MJ, Overmoyer B, Jones SF, Harris JL, Smith DA, Koch KM, Stead A, Mangum S, and Spector NL (2005) Phase I safety, pharmacokinetics, and clinical activity study of lapatinib (GW572016), a reversible dual inhibitor of epidermal growth factor receptor tyrosine kinases, in heavily pretreated patients with metastatic carcinomas. *J Clin Oncol* **23:**5305-5313.

Castellino S, O'Mara M, Koch K, Borts DJ, Bowers GD, and MacLauchlin C (2012) Human metabolism of lapatinib, a dual kinase inhibitor: Implications for hepatotoxicity. *Drug Metab Dispos* **40:**139-150.

Chan ECY, New LS, Chua TB, Yap CW, Ho HK, and Nelson SD (2012) Interaction of lapatinib with cytochrome P450 3A5. *Drug Metab Dispos* **40:**1414-1422.

Chan JCY, Choo DYM, and Chan ECY (2014) Impact of CYP3A5 genetic polymorphism on mechanism-based inactivation by lapatinib, Abstract in: *19th International Society for the Study of Xenobiotics (ISSX) North American and 29th Japanese Society for the Study of Xenobiotics (JSSX) Meeting*, San Francisco, CA.

de Wit D, Gelderblom H, Sparreboom A, den Hartigh J, den Hollander M, Konig-Quartel JM, Hessing T, Guchelaar HJ, and van Erp NP (2014) Midazolam as a phenotyping probe to predict sunitinib exposure in patients with cancer. *Cancer Chemother Pharmacol* **73:**87-96.

Dennison JB, Jones DR, Renbarger JL, and Hall SD (2007) Effect of CYP3A5 expression on vincristine metabolism with human liver microsomes. *J Pharmacol Exp Ther* **321:**553-563.

Dick RA (2018) Refinement of in vitro methods for identification of aldehyde oxidase substrates reveals metabolites of kinase inhibitors. *Drug Metab Dispos* **46:**846-859.

Gomez HL, Doval DC, Chavez MA, Ang PC, Aziz Z, Nag S, Ng C, Franco SX, Chow LW, Arbushites MC, Casey MA, Berger MS, Stein SH, and Sledge GW (2008) Efficacy and safety of lapatinib as first-line therapy for ErbB2-amplified locally advanced or metastatic breast cancer. *J Clin Oncol* **26:**2999-3005.

Goss PE, Smith IE, O'Shaughnessy J, Ejlertsen B, Kaufmann M, Boyle F, Buzdar AU, Fumoleau P, Gradishar W, Martin M, Moy B, Piccart-Gebhart M, Pritchard KI, Lindquist D, Chavarri-Guerra Y, Aktan G, Rappold E, Williams LS, and Finkelstein DM (2013) Adjuvant lapatinib for women with early-stage HER2-positive breast cancer: a randomised, controlled, phase 3 trial. *The Lancet Oncology* **14:**88-96.

Hardy KD, Wahlin MD, Papageorgiou I, Unadkat JD, Rettie AE, and Nelson SD (2014) Studies on the role of metabolic activation in tyrosine kinase inhibitor–dependent hepatotoxicity: Induction of CYP3A4 enhances the cytotoxicity of lapatinib in HepaRG cells. *Drug Metab Dispos* **42:**162-171.

Hesselink DA, van Schaik RH, van der Heiden IP, van der Werf M, Gregoor PJ, Lindemans J, Weimar W, and van Gelder T (2003) Genetic polymorphisms of the CYP3A4, CYP3A5, and MDR-1 genes and pharmacokinetics of the calcineurin inhibitors cyclosporine and tacrolimus. *Clin Pharmacol Ther* **74:**245-254.

Ho HK, Chan JC, Hardy KD, and Chan EC (2015) Mechanism-based inactivation of CYP450 enzymes: a case study of lapatinib. *Drug Metab Rev* **47:**21-28.

Huang W, Lin YS, McConn DJ, 2nd, Calamia JC, Totah RA, Isoherranen N, Glodowski M, and Thummel KE (2004) Evidence of significant contribution from CYP3A5 to hepatic drug metabolism. *Drug Metab Dispos* **32:**1434-1445.

Hustert E, Haberl M, Burk O, Wolbold R, He YQ, Klein K, Nuessler AC, Neuhaus P, Klattig J, Eiselt R, Koch I, Zibat A, Brockmöller J, Halpert JR, Zanger UM, and Wojnowski L (2001) The genetic determinants of the CYP3A5 polymorphism. *Pharmacogenetics* **11:**773-779.

Klees TM, Sheffels P, Thummel KE, and Kharasch ED (2005) Pharmacogenetic determinants of human liver microsomal alfentanil metabolism and the role of cytochrome P450 3A5. *Anesthesiology* **102:**550-556.

Klein K and Zanger UM (2013) Pharmacogenomics of Cytochrome P450 3A4: Recent progress toward the "missing heritability" problem. *Front Genet* **4:**12.

Kuehl P, Zhang J, Lin Y, Lamba J, Assem M, Schuetz J, Watkins PB, Daly A, Wrighton SA, Hall SD, Maurel P, Relling M, Brimer C, Yasuda K, Venkataramanan R, Strom S, Thummel K, Boguski MS, and Schuetz E (2001) Sequence diversity in CYP3A promoters and characterization of the genetic basis of polymorphic CYP3A5 expression. *Nat Genet* **27:**383-391.

Lackey KE (2006) Lessons from the drug discovery of lapatinib, a dual ErbB1/2 tyrosine kinase inhibitor. *Curr Top Med Chem* **6:**435-460.

Lamba JK, Lin YS, Schuetz EG, and Thummel KE (2002) Genetic contribution to variable human CYP3A-mediated metabolism. *Adv Drug Deliv Rev* **54:**1271-1294.

Lamba V, Panetta JC, Strom S, and Schuetz EG (2010) Genetic predictors of interindividual variability in hepatic CYP3A4 expression. *J Pharmacol Exp Ther* **332:**1088-1099.

Li X, Jeso V, Heyward S, Walker GS, Sharma R, Micalizio GC, and Cameron MD (2014) Characterization of T-5 *N*-oxide formation as the first highly selective measure of CYP3A5 activity. *Drug Metab Dispos* **42:**334-342.

Li X, Song X, Kamenecka TM, and Cameron MD (2012) Discovery of a highly selective CYP3A4 inhibitor suitable for reaction phenotyping studies and differentiation of CYP3A4 and CYP3A5. *Drug Metab Dispos* **40:**1803-1809.

Lin YS, Dowling AL, Quigley SD, Farin FM, Zhang J, Lamba J, Schuetz EG, and Thummel KE (2002) Co-regulation of CYP3A4 and CYP3A5 and contribution to hepatic and intestinal midazolam metabolism. *Mol Pharmacol* **62:**162-172.

Lu Y, Fuchs EJ, Hendrix CW, and Bumpus NN (2014) CYP3A5 genotype impacts maraviroc concentrations in healthy volunteers. *Drug Metab Dispos* **42:**1796-1802.

Lu Y, Hendrix CW, and Bumpus NN (2012) Cytochrome P450 3A5 plays a prominent role in the oxidative metabolism of the anti-human immunodeficiency virus drug maraviroc. *Drug Metab Dispos* **40:**2221-2230.

Moy B, Kirkpatrick P, Kar S, and Goss P (2007) Lapatinib. *Nat Rev Drug Discov* **6:**431-432.

Moy B, Rappold E, Williams L, Kelly T, Nicolodi L, Maltzman JD, and Goss PE (2009) Hepatobiliary abnormalities in patients with metastatic cancer treated with lapatinib. *J Clin Oncol* **27:** no. 15_suppl (May 20 2009) 1043-1043.

Parham LR, Briley LP, Li L, Shen J, Newcombe PJ, King KS, Slater AJ, Dilthey A, Iqbal Z, McVean G, Cox CJ, Nelson MR, and Spraggs CF (2015) Comprehensive genome-wide evaluation of lapatinib-induced liver injury yields a single genetic signal centered on known risk allele HLA-DRB1*07:01. *Pharmacogenomics J* **16**:180-185.

Peroukides S, Makatsoris T, Koutras A, Tsamandas A, Onyenadum A, Labropoulou-Karatza C, and Kalofonos H (2011) Lapatinib-induced hepatitis: a case report. *World J Gastroenterol* **17:**2349-2352.

Polli JW, Humphreys JE, Harmon KA, Castellino S, O'Mara MJ, Olson KL, John-Williams LS, Koch KM, and Serabjit-Singh CJ (2008) The role of efflux and uptake transporters in [N-{3-chloro-4-[(3-fluorobenzyl)oxy]phenyl}-6-[5-({[2-(methylsulfonyl)ethyl]amino }methyl)-2-furyl]-4-quinazolinamine (GW572016, lapatinib) disposition and drug interactions. *Drug Metab Dispos* **36:**695-701.

Roy SK, Korzekwa KR, Gonzalez FJ, Moschel RC, and Dolan ME (1995) Human liver oxidative metabolism of O6-benzylguanine. *Biochem Pharmacol* **50:**1385-1389.

Rusnak DW, Affleck K, Cockerill SG, Stubberfield C, Harris R, Page M, Smith KJ, Guntrip SB, Carter MC, Shaw RJ, Jowett A, Stables J, Topley P, Wood ER, Brignola PS, Kadwell SH, Reep BR, Mullin RJ, Alligood KJ, Keith BR, Crosby RM, Murray DM, Knight WB, Gilmer TM, and Lackey K (2001) The characterization of novel, dual ErbB-2/EGFR, tyrosine kinase inhibitors: potential therapy for cancer. *Cancer Res* **61:**7196-7203.

Schaid DJ, Spraggs CF, McDonnell SK, Parham LR, Cox CJ, Ejlertsen B, Finkelstein DM, Rappold E, Curran J, Cardon LR, and Goss PE (2014) Prospective validation of HLA-DRB1*07:01 allele carriage as a predictive risk factor for lapatinib-induced liver injury. *J Clin Oncol* **32:**2296-2303.

Sorich MJ, Mutlib F, van Dyk M, Hopkins AM, Polasek TM, Marshall JC, Rodrigues AD, and Rowland A (2019) Use of physiologically based pharmacokinetic modeling to identify physiological and molecular characteristics driving variability in axitinib

exposure: A fresh approach to precision dosing in oncology. *J Clin Pharmacol* **59:**872-879.

Spraggs CF, Budde LR, Briley LP, Bing N, Cox CJ, King KS, Whittaker JC, Mooser VE, Preston AJ, Stein SH, and Cardon LR (2011) HLA-DQA1*02:01 is a major risk factor for lapatinib-induced hepatotoxicity in women with advanced breast cancer. *J Clin Oncol* **29:**667-673.

Spraggs CF, Parham LR, Hunt CM, and Dollery CT (2012) Lapatinib-induced liver injury characterized by class II HLA and Gilbert's Syndrome genotypes. *Clin PharmacolTher* **91:**647-652.

Takakusa H, Wahlin MD, Zhao C, Hanson KL, New LS, Chan ECY, and Nelson SD (2011) Metabolic intermediate complex formation of human cytochrome P450 3A4 by lapatinib. *Drug Metab Dispos* **39:**1022-1030.

Teng WC, Oh JW, New LS, Wahlin MD, Nelson SD, Ho HK, and Chan ECY (2010) Mechanism-based inactivation of cytochrome P450 3A4 by lapatinib. *Mol Pharmacol* **78:**693-703.

Teo YL, Saetaew M, Chanthawong S, Yap YS, Chan EC, Ho HK, and Chan A (2012) Effect of CYP3A4 inducer dexamethasone on hepatotoxicity of lapatinib: clinical and in vitro evidence. *Breast Cancer Res Treat* **133:**703-711.

Towles JK, Clark RN, Wahlin MD, Uttamsingh V, Rettie AE, and Jackson KD (2016) Cytochrome P450 3A4 and CYP3A5-catalyzed bioactivation of lapatinib. *Drug Metab Dispos* **44:**1584-1597.

Tseng E, Fate GD, Walker GS, Goosen TC, and Obach RS (2018) Biosynthesis and Identification of metabolites of maraviroc and their use in experiments to

delineate the relative contributions of cytochrome P4503A4 versus 3A5. *Drug Metab Dispos* **46:**493-502.

Tseng E, Walsky RL, Luzietti RA, Jr., Harris JJ, Kosa RE, Goosen TC, Zientek MA, and Obach RS (2014) Relative contributions of cytochrome CYP3A4 versus CYP3A5 for CYP3A-cleared drugs assessed in vitro using a CYP3A4-selective inactivator (CYP3cide). *Drug Metab Dispos* **42:**1163-1173.

Walsky RL and Obach RS (2004) Validated assays for human cytochrome P450 activities. *Drug Metab Dispos* **32:**647-660.

Walsky RL, Obach RS, Hyland R, Kang P, Zhou S, West M, Geoghegan KF, Helal CJ, Walker GS, Goosen TC, and Zientek MA (2012) Selective mechanism-based inactivation of CYP3A4 by CYP3cide (PF-04981517) and its utility as an in vitro tool for delineating the relative roles of CYP3A4 versus CYP3A5 in the metabolism of drugs. *Drug Metab Dispos* **40:**1686-1697.

Wang D, Guo Y, Wrighton SA, Cooke GE, and Sadee W (2011) Intronic polymorphism in CYP3A4 affects hepatic expression and response to statin drugs. *Pharmacogenomics J* **11:**274-286.

Wang D and Sadee W (2016) CYP3A4 intronic SNP rs35599367 (CYP3A4*22) alters RNA splicing. *Pharmacogenet Genomics* **26:**40-43.

Wrighton SA and Stevens JC (1992) The human hepatic cytochromes P450 involved in drug metabolism. *Crit Rev Toxicol* **22:**1-21.

Yang X, Zhang B, Molony C, Chudin E, Hao K, Zhu J, Gaedigk A, Suver C, Zhong H, Leeder JS, Guengerich FP, Strom SC, Schuetz E, Rushmore TH, Ulrich RG, Slatter JG, Schadt EE, Kasarskis A, and Lum PY (2010) Systematic genetic and

genomic analysis of cytochrome P450 enzyme activities in human liver. *Genome Res* **20:**1020-1036.

Zanger UM and Schwab M (2013) Cytochrome P450 enzymes in drug metabolism: regulation of gene expression, enzyme activities, and impact of genetic variation. *Pharmacol Ther* **138:**103-141.

Zientek MA, Goosen TC, Tseng E, Lin J, Bauman JN, Walker GS, Kang P, Jiang Y, Freiwald S, Neul D, and Smith BJ (2016) In vitro kinetic characterization of axitinib metabolism. *Drug Metab Dispos* **44:**102-114.

Funding

This research is funded by the National Cancer Institute of the National Institutes of Health (K01CA190711). Research reported here is solely the responsibility of the authors and does not necessarily represent the official views of the National Institutes of Health.

Figure Legends

Figure 1. Measurement of CYP3A activity by midazolam 1´-hydroxylation and CYP3A5-selective activity by T-5 *N*-oxidation in genotyped human liver microsomes. (A) Midazolam (2.5 μM) was incubated with single-donor human liver microsomes (0.03 mg protein/ml) supplemented with NADPH-generating system for 4 minutes. (B) T-5 (5 μM) was incubated with single-donor human liver microsomes (0.1 mg protein/ml) supplemented with NADPH-generating system for 15 minutes. Formation of 1´-hydroxymidazolam and T-5 *N*-oxide was measured by LC-MS/MS analysis. Each point is the mean of three experiments performed in triplicate each. *CYP3A5*3/*3* donors, n = 5; *CYP3A5*1/*3* donors, n = 3; *CYP3A5*1/*1* donors, n = 4. Metabolite formation was compared across *CYP3A5* genotypes by one-way ANOVA using GraphPad Prism 7 software.

Figure 2. Lapatinib *O*-debenzylation and formation of quinoneimine-GSH conjugates in genotyped human liver microsomes. Lapatinib (5 μM) was incubated with single-donor human liver microsomes (0.1 mg protein/ml) supplemented with NADPH-generating system for 20 minutes. Formation of debenzylated lapatinib, M1 (A) and quinoneimine-GSH conjugates (B) was measured by LC-MS/MS analysis. Relative metabolite levels are reported as peak area ratio (metabolite peak area/internal standard peak area). Each point is the mean of two to three experiments performed in triplicate each. *CYP3A5*3/*3* donors, n = 5; *CYP3A5*1/*3* donors, n = 2; *CYP3A5*1/*1* donors, n = 4.

Metabolite formation was compared across *CYP3A5* genotypes by one-way ANOVA using GraphPad Prism 7 software.

Figure 3. Correlation of lapatinib bioactivation with CYP3A activity in genotyped human liver microsomes. Formation of M1 (A-B) and quinoneimine-GSH conjugates (C-D) was analyzed for correlation with midazolam 1´-hydroxylation (A, C) and T-5 *N*-oxidation (B, D). The correlation of quinoneimine-GSH conjugate vs. M1 formation was analyzed to assess the relationship between bioactivation steps (E). The number of total human liver donors was 11. Each point is the mean from two to three experiments performed in triplicate each. Linear regression analysis was performed to determine r^2 and Pearson r correlation using GraphPad Prism 7 software.

Figure 4. Effect of CYP3A and CYP3A4-selective inhibition on lapatinib M1 formation in a CYP3A5 expresser vs. non-expresser. Lapatinib (5 μM) was incubated with single-donor human liver microsomes (0.1 mg protein/ml) supplemented with NADPH-generating system for 20 minutes with and without CYP3A4-selective inhibitor CYP3cide (2 μM) or CYP3A inhibitor ketoconazole (1 μM). Incubations were carried out with (A) pooled human liver microsomes from 150-donors (mixed gender) and human liver microsomes from individual genotyped donors: (B) *CYP3A5*3/*3*, n = 3: 710252 (male), 719253 (male), 710237 (male); (C) *CYP3A5*1/*1*, n = 4: HH860 (female), HH867 (male), HH785 (male), 710272 (female). Formation of lapatinib M1 was measured by LC-MS/MS analysis. Control rates of M1 formation are reported in Table 1. Percent control metabolite formation was determined by comparison to vehicle

control incubations without inhibitor. Two independent experiments were performed in triplicate each to assess reproducibility. Shown are the results from a representative experiment. Bars indicate the means, and error bars denote the standard deviation.

Figure 5. Midazolam 1´-hydroxylation, T-5 *N*-oxidation, and lapatinib *O*-debenzylation in pooled human hepatocytes. Genotyped human hepatocytes were from a pool of three donors each. (A) Midazolam (2.5 μM) and (B) T-5 (5 μM) were incubated with hepatocytes (0.5 x 10^6 cells/ml) in suspension for 30 minutes. (C) Lapatinib (10 μM) was incubated with hepatocytes (0.5 x 10^6 cells/ml) in suspension for 2 hours. Formation of 1´-hydroxymidazolam, T-5 *N*-oxide, and lapatinib M1 was measured by LC-MS/MS analysis. Relative levels of M1 were determined by the ratio of M1 to lapatinib peak areas and normalized to *CYP3A5*1/*1* donors. Each point is from a single experiment performed in replicate (2-4). The mean is indicated by the line, and errors are the standard deviation.

Figure 6. CYP3A and CYP3A5-selective activity in genotyped single-donor human hepatocytes. (A) Midazolam (2.5 μM) and (B) T-5 (5 μM) were incubated with hepatocytes (0.5 x 10^6 cells/ml) in suspension for 30 minutes. Formation of 1´-hydroxymidazolam (A) and T-5 *N*-oxide (B) was measured by LC-MS/MS analysis. Results are the mean values for each donor from experiments performed in triplicate. *CYP3A5*3/*3* donors, n = 8; *CYP3A5*1/*3* donors, n = 5; *CYP3A5*1/*1* donors, n = 2. Comparison one-way ANOVA (GraphPad Prism 7).

Figure 7. Lapatinib M1 formation in genotyped single-donor human hepatocytes. Lapatinib (10 μM) was incubated with hepatocytes (0.5 x 10^6 cells/ml) in suspension for 2.2 hours. Formation of lapatinib M1 was quantified by LC-MS/MS analysis using a standard curve. Results are the mean values for each donor from experiments performed in triplicate. *CYP3A5*3/*3* donors, n = 8; *CYP3A5*1/*3* donors, n = 5; *CYP3A5*1/*1* donors, n = 2. M1 formation is plotted by *CYP3A5* genotype.

Figure 8. Correlation of lapatinib M1 formation with CYP3A- and CYP3A5-selective activity in genotyped single-donor human hepatocytes. Formation of M1 was analyzed for correlation with midazolam 1´-hydroxylation (A) and T-5 *N*-oxidation (B). Results are the mean values for each donor from experiments performed in triplicate. The total human liver donors was n = 15. *CYP3A5*3/*3* donors, n = 8; *CYP3A5*1/*3* donors, n = 5; *CYP3A5*1/*1* donors, n = 2. Linear regression analysis was performed to determine r^2 and Pearson r correlation using GraphPad Prism 7.

Figure 9. Lapatinib quinoneimine-GSH conjugate formation in genotyped human hepatocytes and correlation with CYP3A- and CYP3A5-selective activity. Relative levels of quinoneimine-GSH conjugates (peak area/internal standard peak area) were measured by LC-MS/MS analysis. Formation of quinoneimine-GSH conjugates was analyzed for correlation with midazolam 1´-hydroxylation (A) and T-5 *N*-oxidation (B). Results are the mean values for each donor from experiments performed in triplicate. The total human liver donors with detectable quinoneimine-GSH conjugates was eight. *CYP3A5*3/*3* donors, n = 4; *CYP3A5*1/*3* donors, n = 3; *CYP3A5*1/*1* donor, n = 1.

Linear regression analysis was performed to determine r^2 and Pearson r correlation using GraphPad Prism 7.

Figure 10. Effect of CYP3A and CYP3A4-selective inhibition on lapatinib M1 formation in a CYP3A5 expresser vs. non-expresser. Lapatinib (10 μM) was incubated with hepatocytes (0.5 x 10^6 cells/ml) in suspension for 2.2 hours with and without CYP3A4-selective inhibitor CYP3cide (2 μM) or CYP3A inhibitor ketoconazole (1 μM). Relative levels of lapatinib M1 were measured by LC-MS/MS analysis. Results are the mean and standard deviation from a single experiment performed in duplicate or triplicate. (A) Donor JYS, CYP3A5 non-expresser (*CYP3A5*3/*3*). (B) Donor OWY, CYP3A5 expresser (*CYP3A5*1/*3*).

Figure 11. Lapatinib metabolism: CYP3A-mediated bioactivation vs. aldehyde oxidase-mediated pathway

DMD Fast Forward. Published on September 6, 2019 as DOI: 10.1124/dmd.119.088823
This article has not been copyedited and formatted. The final version may differ from this version.

Table 1

Estimation of CYP3A5 contribution to lapatinib *O*-debenzylation (M1 formation) in human liver microsomes from *CYP3A5*-genotyped donors

HLM	M1 formation (pmol/min/mg protein)[a]	% of Control +CYP3cide	% of Control +Ketoconazole	Estimated % CYP3A5 Contribution[b]	*P*
*CYP3A5*1/*1*					
HH860	68 ± 2	28 ± 7	9 ± 1	20	
HH867	37 ± 3	42 ± 4	11 ± 4	31	
HH785	50 ± 11	42 ± 3	13 ± 2	29	
710272	103 ± 8	40 ± 4	14 ± 5	26	
Mean	**65 ± 29**	**38 ± 7**	**12 ± 3**	**26 ± 5**	
*CYP3A5*3/*3*					
710252	79 ± 2	19 ± 2	9 ± 1	10	
710253	59 ± 6	14 ± 4	8 ± 2	6	
710237	14 ± 2	17 ± 6	9 ± 6	8	
Mean	**50 ± 33**	**16 ± 2**	**8 ± 1**	**8 ± 2**	0.0022[c]
Pooled HLM	50 ± 5	25 ± 1	9 ± 3	16	

[a] Formation of debenzylated lapatinib (M1) was quantified by LC-MS/MS analysis using an authentic chemical standard curve, and rates were calculated from control incubations without inhibitor. Values shown are the mean ± standard deviation (SD) of triplicate determinations. “Mean” indicates the mean ± SD rates of M1 formation for *CYP3A5*1/*1* donors (n = 4) and *CYP3A5*3/*3* donors (n = 3).

[b] Mean percentage (%) CYP3A5 contribution was estimated based on the difference between inhibition by CYP3cide and ketoconazole.

[c] Mean percentage (%) CYP3A5 contribution was compared between *CYP3A5*1/*1* donors (n = 4) and *CYP3A5*3/*3* donors (n = 3) by unpaired t-test using GraphPad Prism 7 software.

DMD Fast Forward. Published on September 6, 2019 as DOI: 10.1124/dmd.119.088823
This article has not been copyedited and formatted. The final version may differ from this version.

Figures

Figure 1

A.

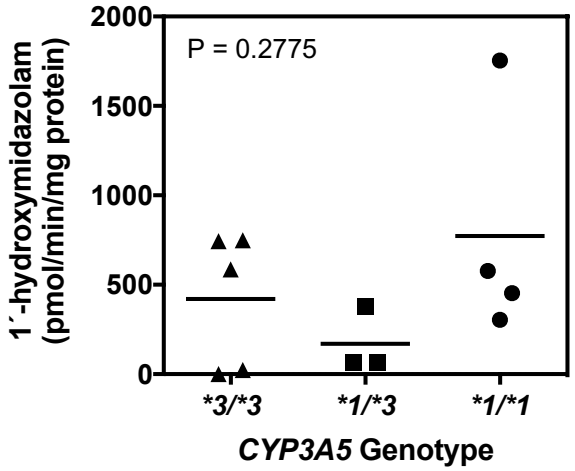

B.

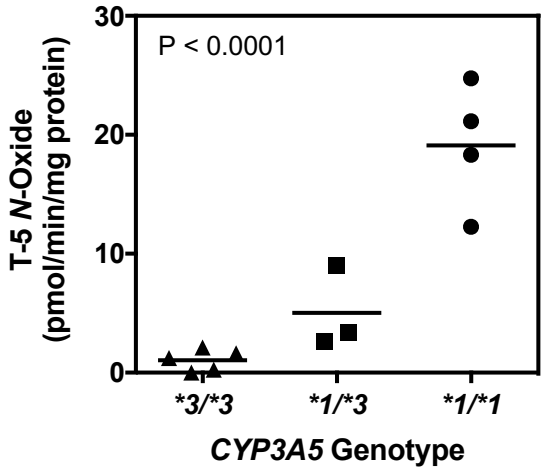

DMD Fast Forward. Published on September 6, 2019 as DOI: 10.1124/dmd.119.088823
This article has not been copyedited and formatted. The final version may differ from this version.

Figure 2

A.

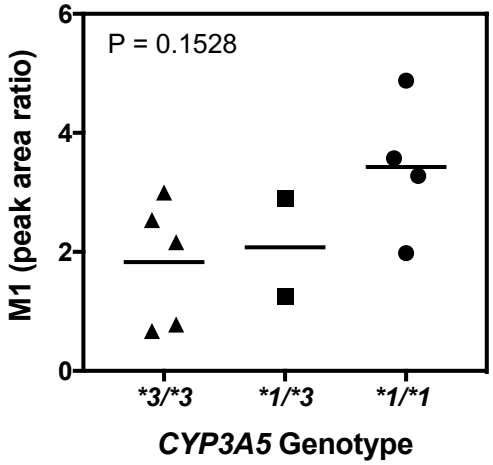

B.

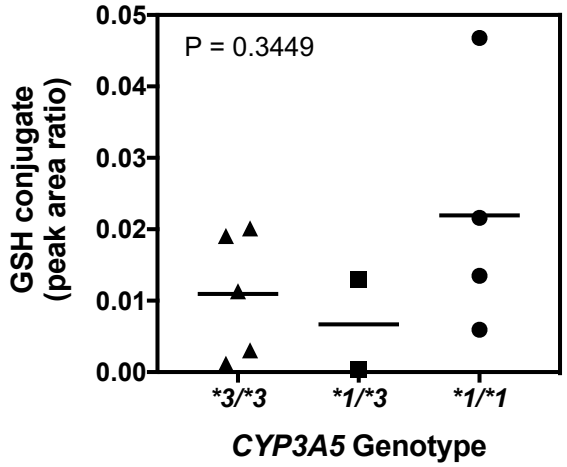

DMD Fast Forward. Published on September 6, 2019 as DOI: 10.1124/dmd.119.088823
This article has not been copyedited and formatted. The final version may differ from this version.

Figure 3

A.

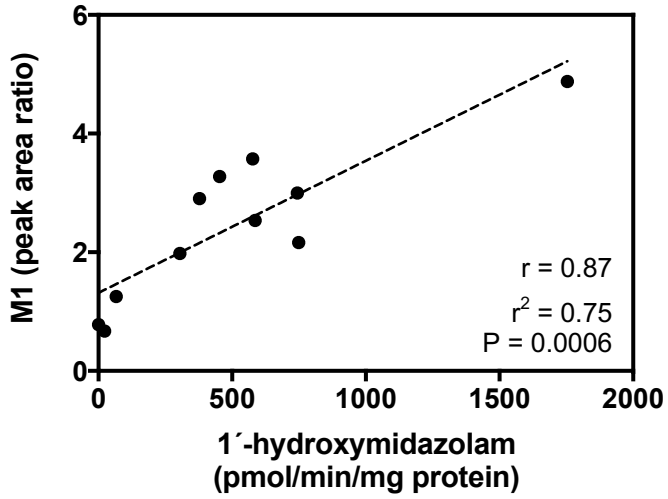

B.

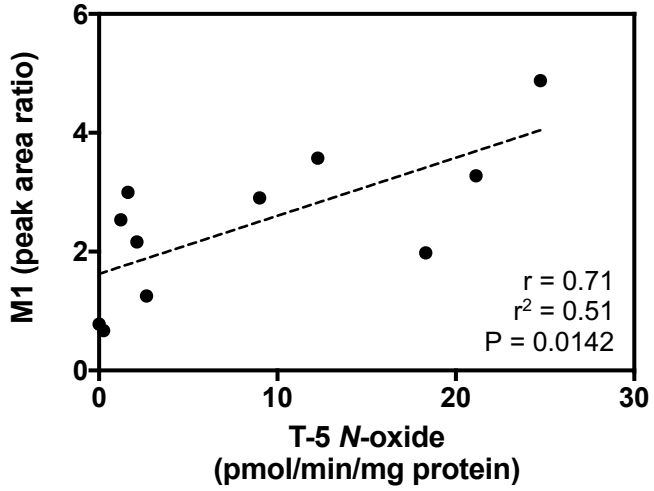

DMD Fast Forward. Published on September 6, 2019 as DOI: 10.1124/dmd.119.088823
This article has not been copyedited and formatted. The final version may differ from this version.

C.

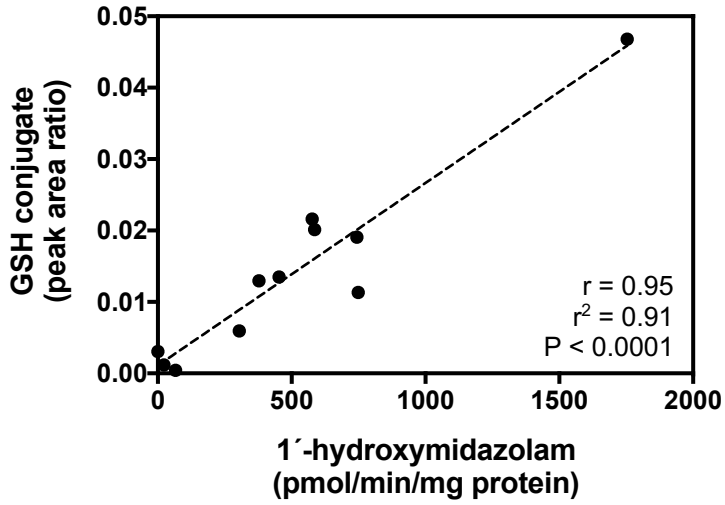

D.

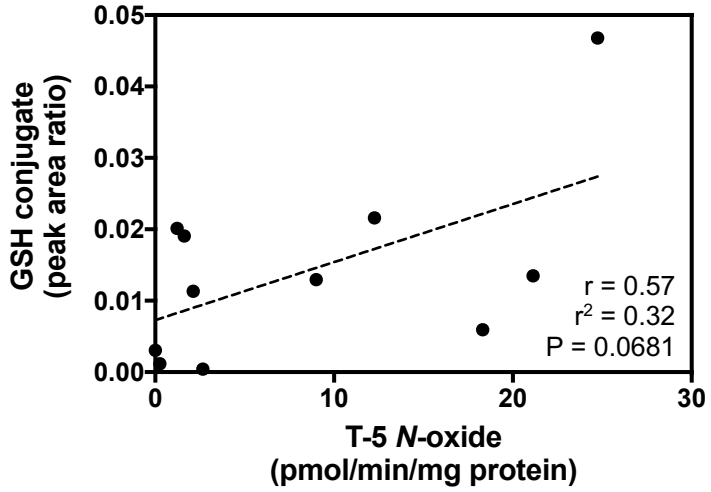

DMD Fast Forward. Published on September 6, 2019 as DOI: 10.1124/dmd.119.088823
This article has not been copyedited and formatted. The final version may differ from this version.

E.

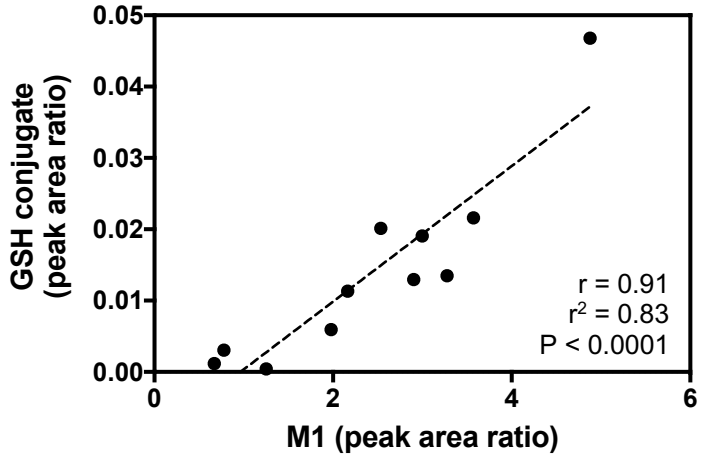

DMD Fast Forward. Published on September 6, 2019 as DOI: 10.1124/dmd.119.088823
This article has not been copyedited and formatted. The final version may differ from this version.

Figure 4.

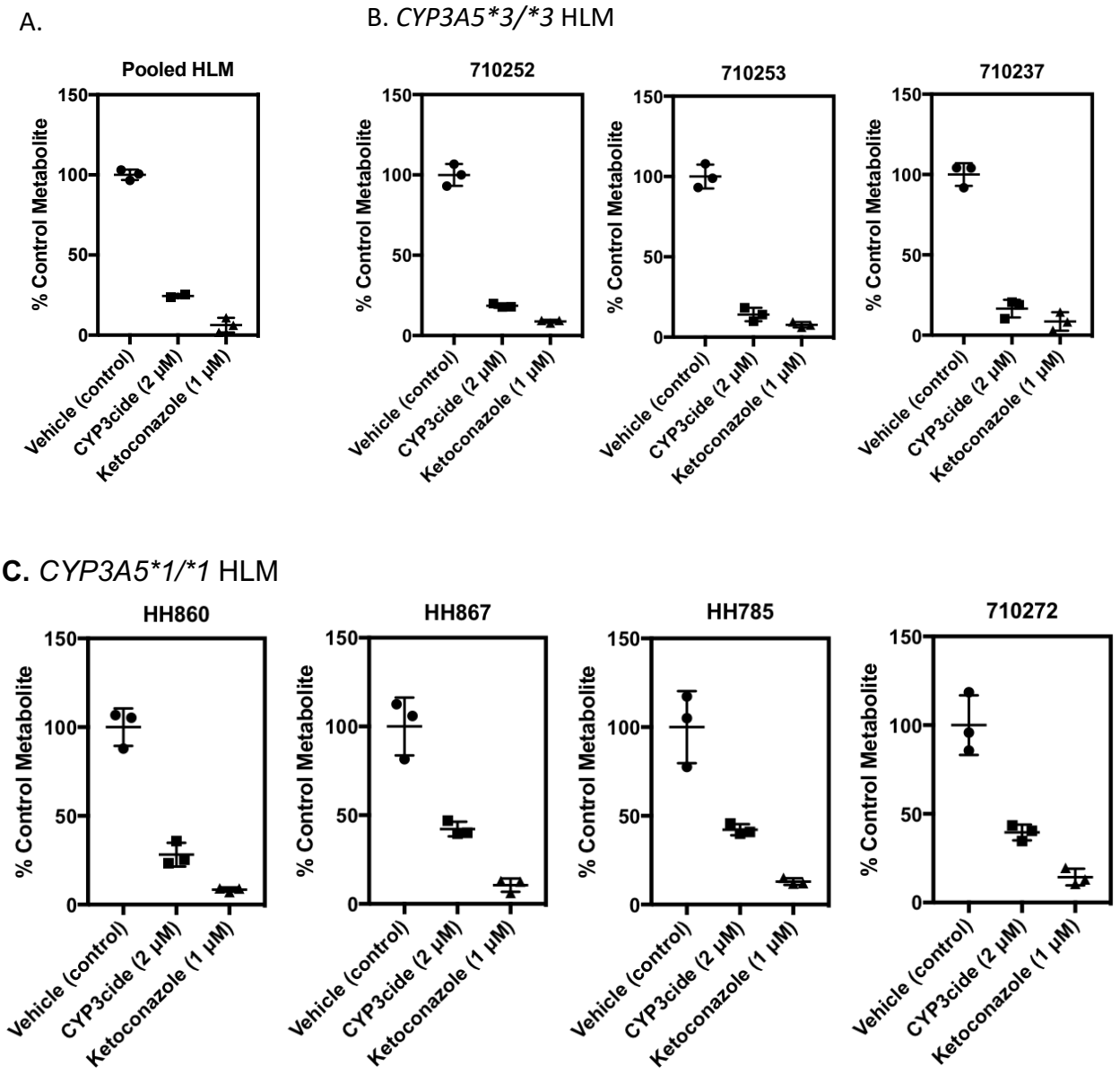

DMD Fast Forward. Published on September 6, 2019 as DOI: 10.1124/dmd.119.088823
This article has not been copyedited and formatted. The final version may differ from this version.

Figure 5

A.

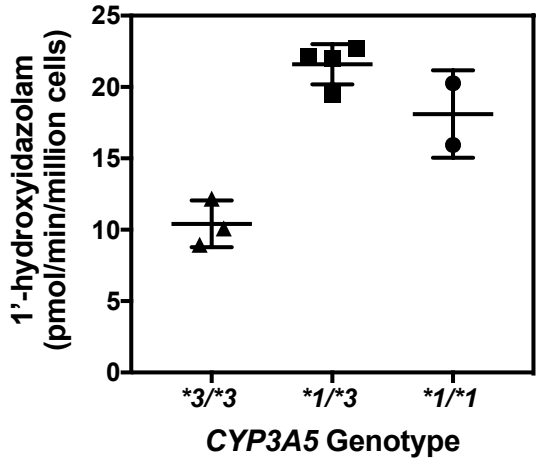

B.

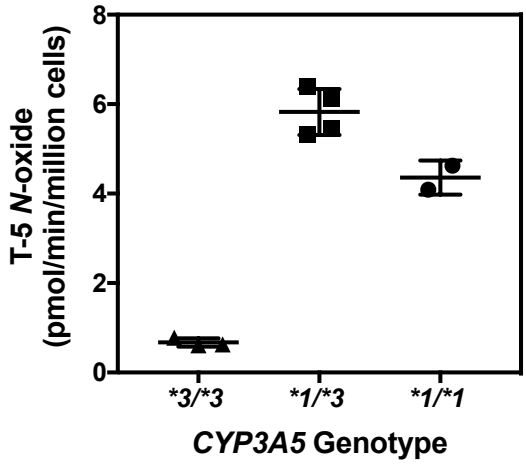

DMD Fast Forward. Published on September 6, 2019 as DOI: 10.1124/dmd.119.088823
This article has not been copyedited and formatted. The final version may differ from this version.

C.

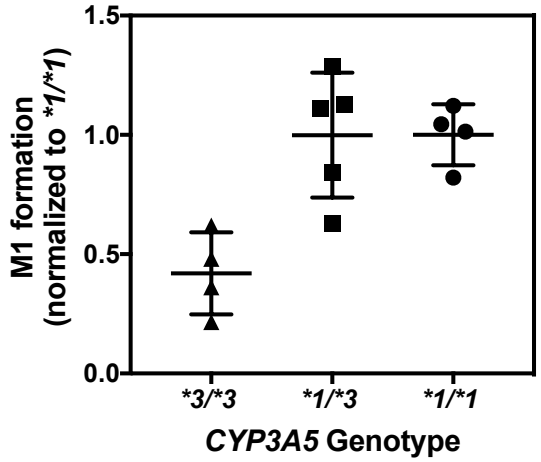

DMD Fast Forward. Published on September 6, 2019 as DOI: 10.1124/dmd.119.088823
This article has not been copyedited and formatted. The final version may differ from this version.

Figure 6

A.

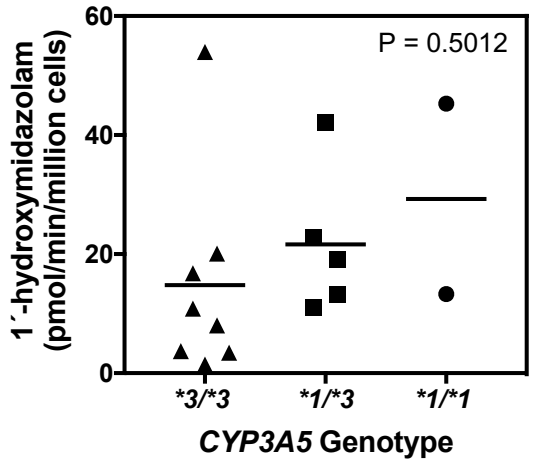

B.

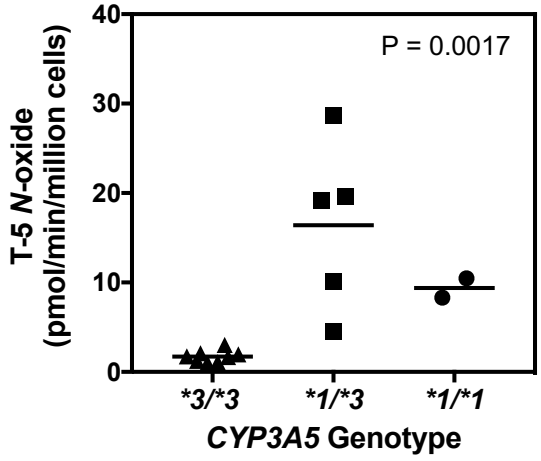

DMD Fast Forward. Published on September 6, 2019 as DOI: 10.1124/dmd.119.088823
This article has not been copyedited and formatted. The final version may differ from this version.

Figure 7

A.

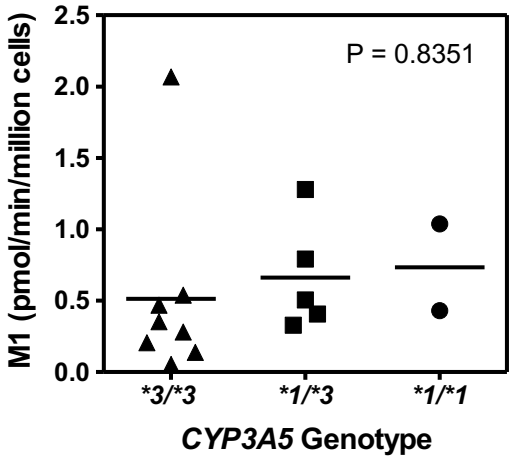

DMD Fast Forward. Published on September 6, 2019 as DOI: 10.1124/dmd.119.088823
This article has not been copyedited and formatted. The final version may differ from this version.

Figure 8

A.

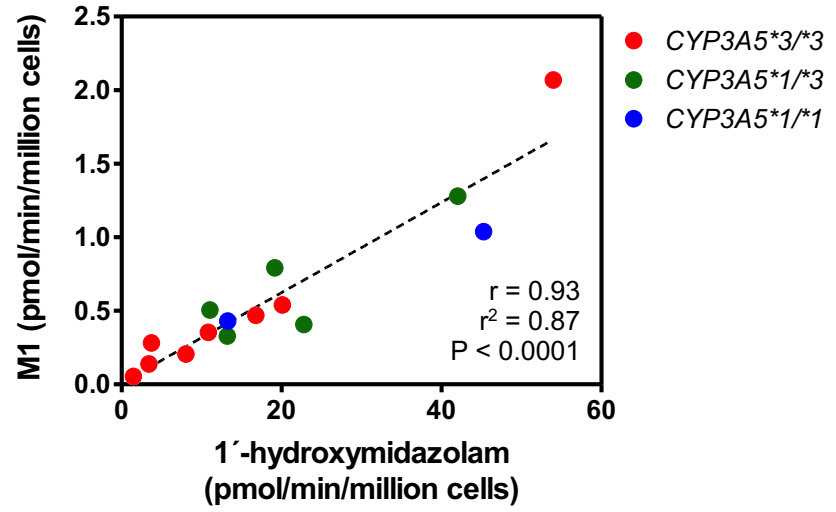

B.

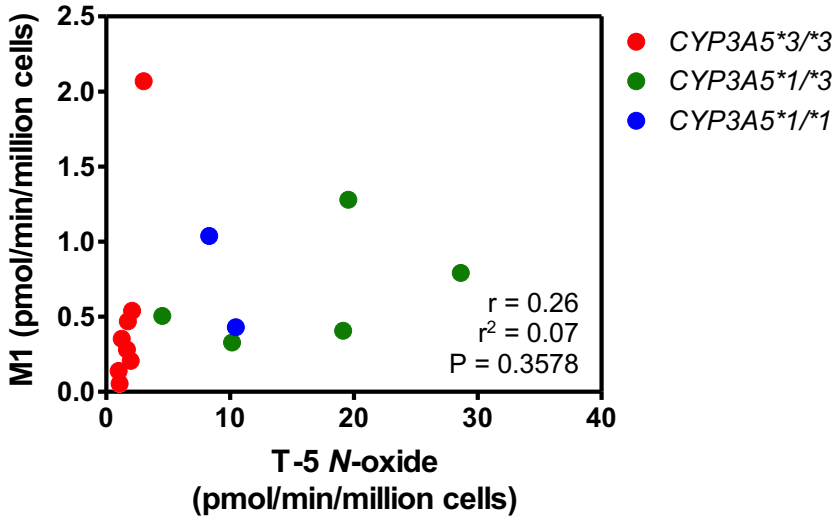

DMD Fast Forward. Published on September 6, 2019 as DOI: 10.1124/dmd.119.088823
This article has not been copyedited and formatted. The final version may differ from this version.

Figure 9

A.

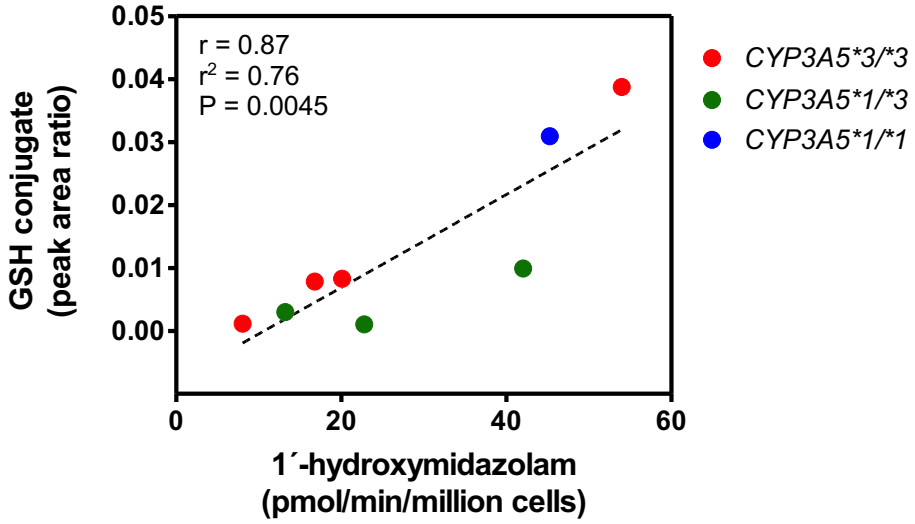

B.

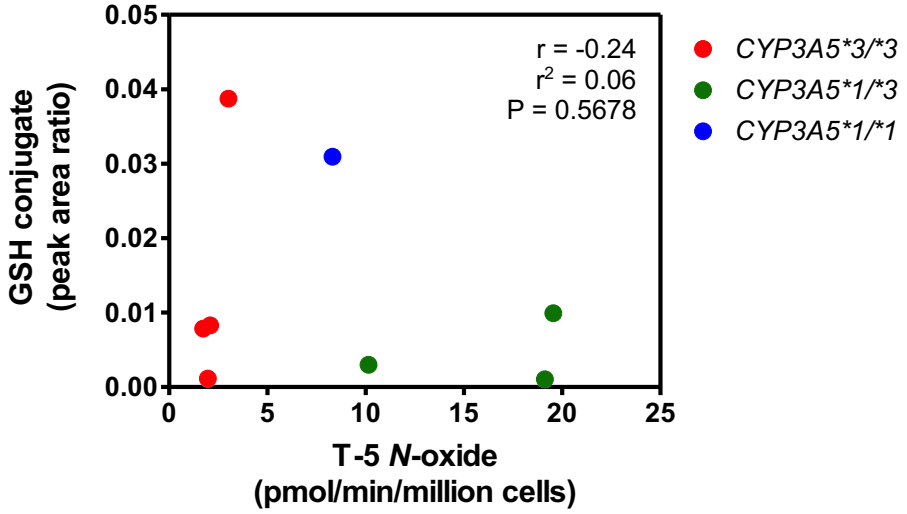

DMD Fast Forward. Published on September 6, 2019 as DOI: 10.1124/dmd.119.088823
This article has not been copyedited and formatted. The final version may differ from this version.

Figure 10

A.

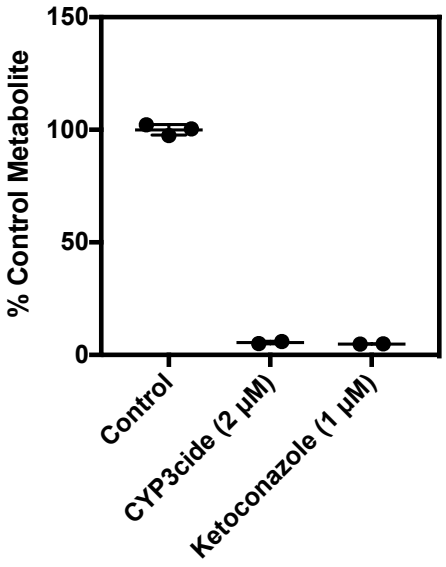

B.

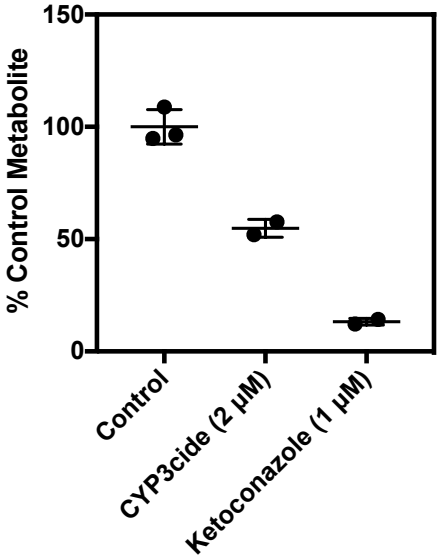

DMD Fast Forward. Published on September 6, 2019 as DOI: 10.1124/dmd.119.088823
This article has not been copyedited and formatted. The final version may differ from this version.

Figure 11